CHAPTER 17
HYDRAULIC DESIGN OF SPILLWAYS

H. Wayne Coleman

C. Y. Wei

James E. Lindell
Harza Engineering Company
Chicago, Illinois

17.1 INTRODUCTION

The spillway is among the most important structures of a dam project. It provides the project with the ability to release excess or flood water in a controlled or uncontrolled manner to ensure the safety of the project. It is of paramount importance for the spillway facilities to be designed with sufficient capacity to avoid overtopping of the dam, especially when an earthfill or rockfill type of dam is selected for the project. In cases where safety of the inhabitants downstream is a key consideration during development of the project, the spillway should be designed to accommodate the probable maximum flood. Many types of spillways can be considered with respect to cost, topographic conditions, dam height, foundation geology, and hydrology. The spillways discussed in this chapter include overflow, overfall, side-channel, orifice, morning-glory, labyrinth, siphon, tunnel, and chute spillways A section on design of spillways that considers cavitation and aeration also is included.

17.2 OVERFLOW SPILLWAY

An *overflow spillway* can be gated or ungated, and it normally provides for flow over a gravity dam section. The flow remains in contact with the spillways surface (except for possible aeration ramps) from the crest of the dam to the vicinity of its base. The hydraulic characteristics are defined as follows:

1. Determine design head H_o. Normally, H_o is 75 to 80% of maximum head H_{max}.
2. Use the depth from the crest to ground surface P to find the basic discharge coefficient C_o from Fig. 17.1.
3. Find discharge coefficient C for the full range of heads from Fig. 17.2.

4. Correct discharge coefficient C for the sloping upstream face from Fig. 17.3. The sloping upstream face is normally for structural stability, not hydraulic efficiency.

5. Correct discharge coefficient C for the downstream apron from Fig. 17.4.

6. Correct discharge coefficient C for tailwater submergence from Fig. 17.5

7. Define the shape of the pier nose. Normally, use Type 3 or 3A from Fig. 17.6.

8. Check the minimum crest pressure from Fig. 17.7 or 17.8. If the minimum pressure is below $-1/2$ atmosphere, increase H_o and start over.

9. Define the crest shape from Fig. 17.9(a) and (b).

10. Determine the effective crest length for the full range of heads from

$$L = L' - 2(NK_p + K_a)\, H_e \qquad (17.1)$$

where: L = effective length of crest, L' = net length of crest, N = number of piers, K = pier contraction coefficient, K_a = abutment contraction coefficient, and H_e = total head on crest.

The following are values of the pier contraction coefficient

	K_p
For square-nosed piers with corners rounded on a radius equal to approximately 0.1 of the pier thickness	0.02
for round-nosed piers	0.01
for pointed-nose piers	0.00

The following are values of the abutment contraction coefficient

	K_a
for square abutments with headwall at 90° to the direction of flown	0.20
for rounded abutments with headwall at 90° to the direction of flow when $0.5H_o > r > 0.15H_o$	0.10
for rounded abutments, where $r > 0.5H_o$, and the headwall is placed no more than 45° to the direction of flow, where r = radius of the abutment rounding.	0.00

11. Determine the discharge rating curve from

$$Q = C\, L\, H_e^{3/2} \qquad (17.2)$$

Exhibits 17.1 and 17.2 illustrate overflow spillings for hydroelectric projects.

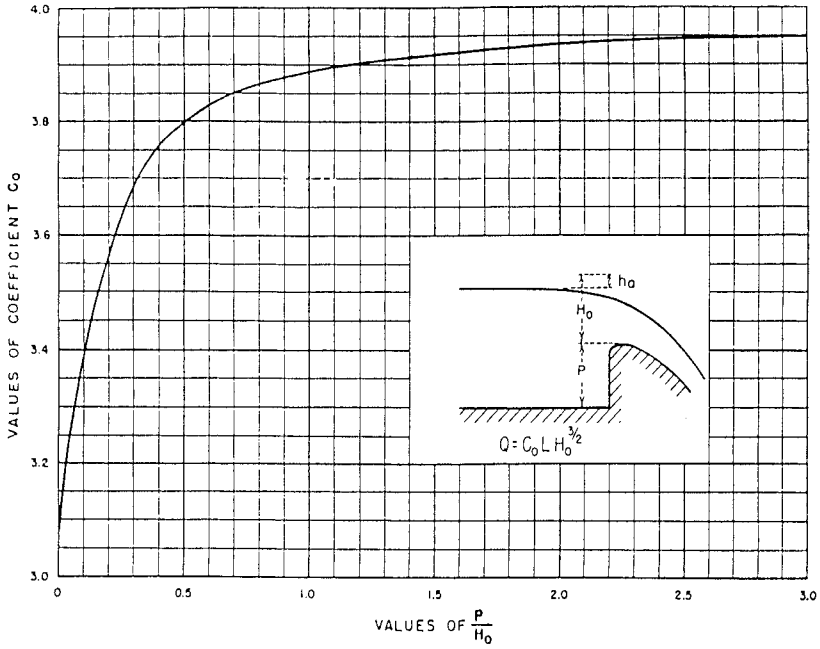

FIGURE 17.1 Discharge coefficients for a vertical-faced ogee crest. (USBR, 1987).

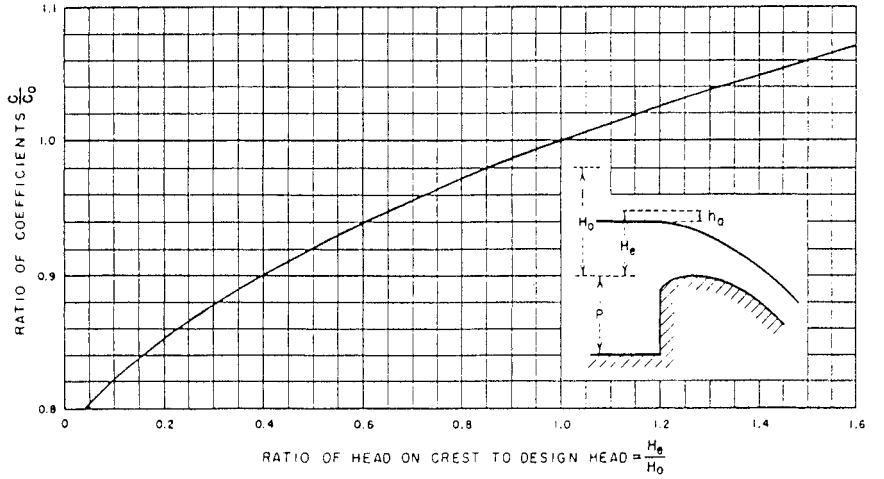

FIGURE 17.2 Coefficient of discharge for other than the design head. (USBR, 1987).

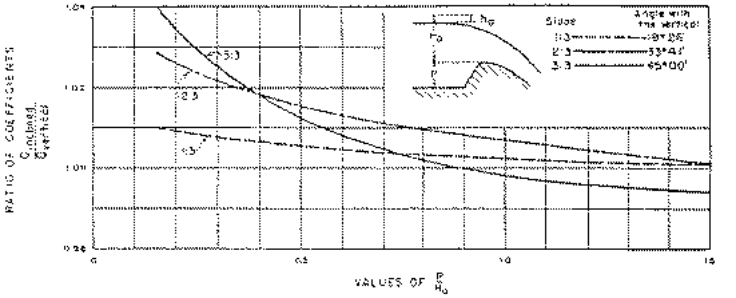

FIGURE 17.3 Coefficient of discharge for an ogee-shaped crest with a sloping upstream face. (USBR, 1987)

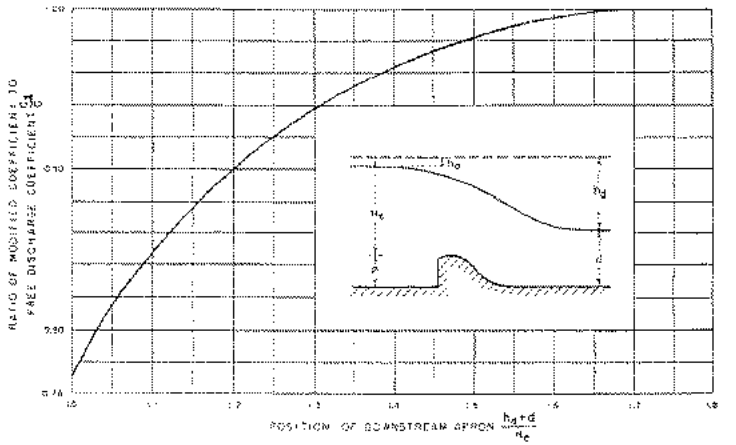

FIGURE 17.4 Ratio of discharge coefficients associated with the apron effect. (USBR, 1987).

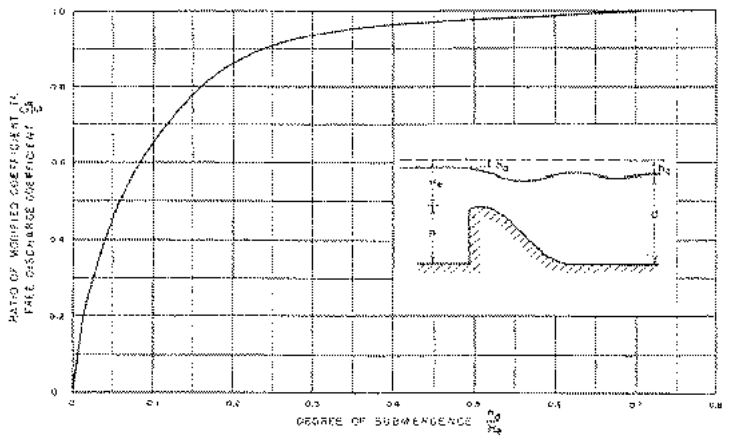

FIGURE 17.5 Ratio of discharge coefficients associated with the tailwater effect. (USBR, 1987).

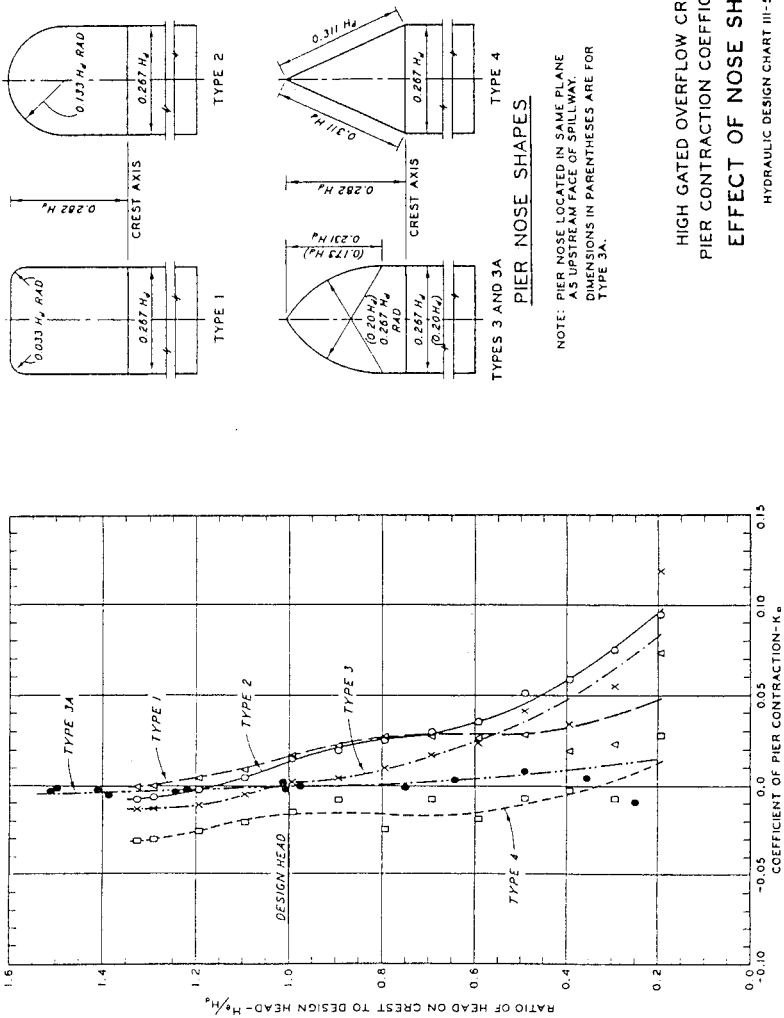

FIGURE 17.6 Pier-contraction coefficients for high-gated overflow crests. (USACE, 1988)

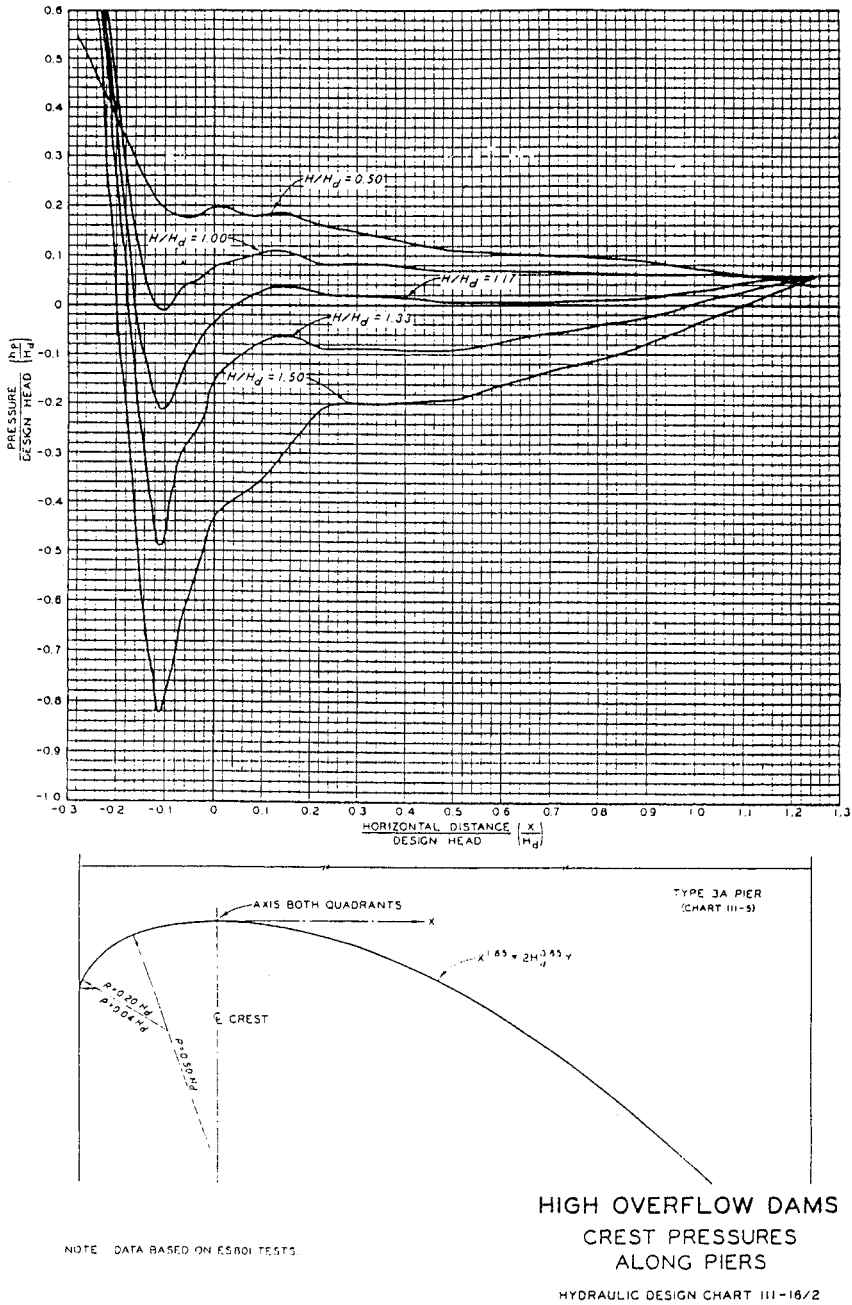

FIGURE 17.7 Crest pressures along piers (Type 3A) for high-overflow dams. (USACE, 1988)

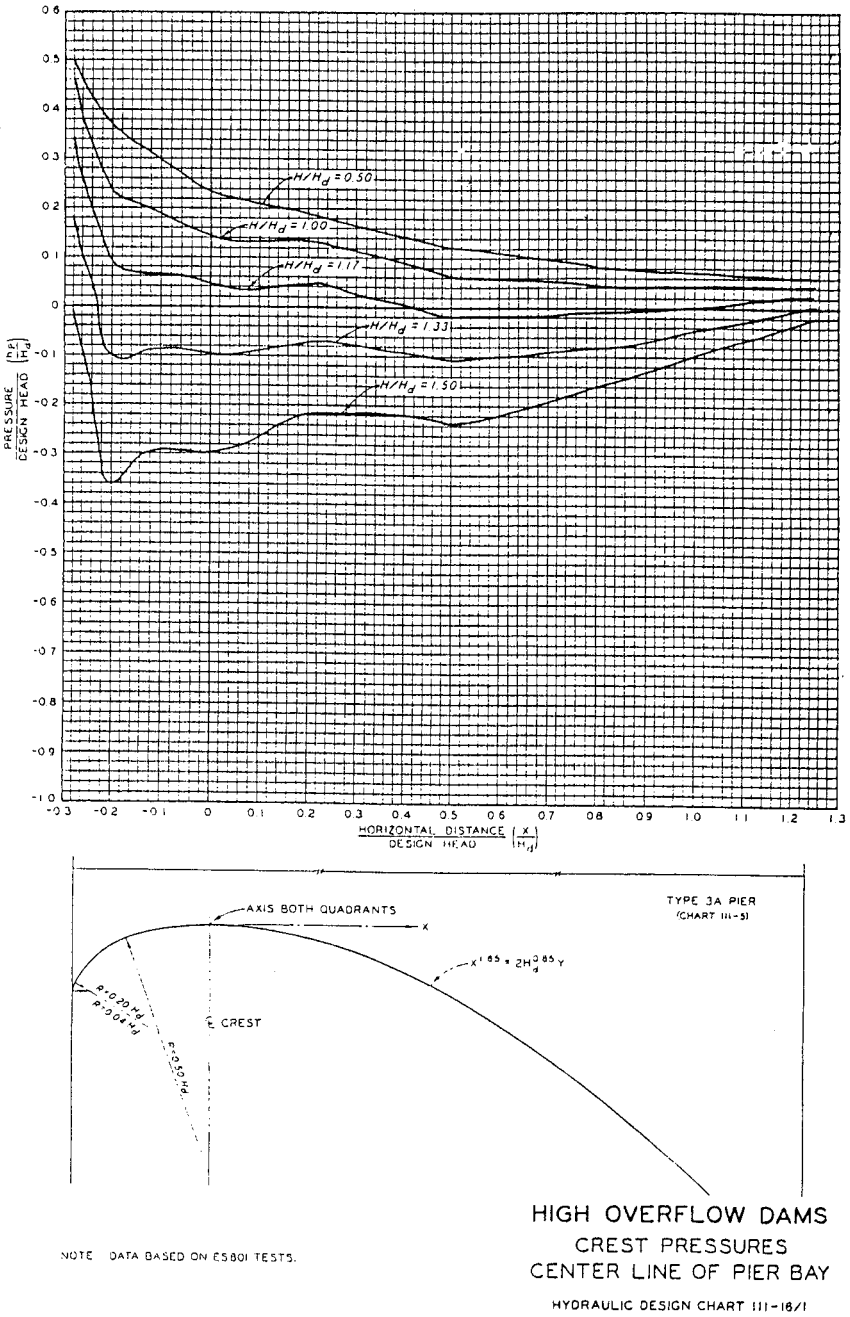

FIGURE 17.8 Crest pressures along the centerline of a pier (Type 3A) bay. (USACE, 1988)

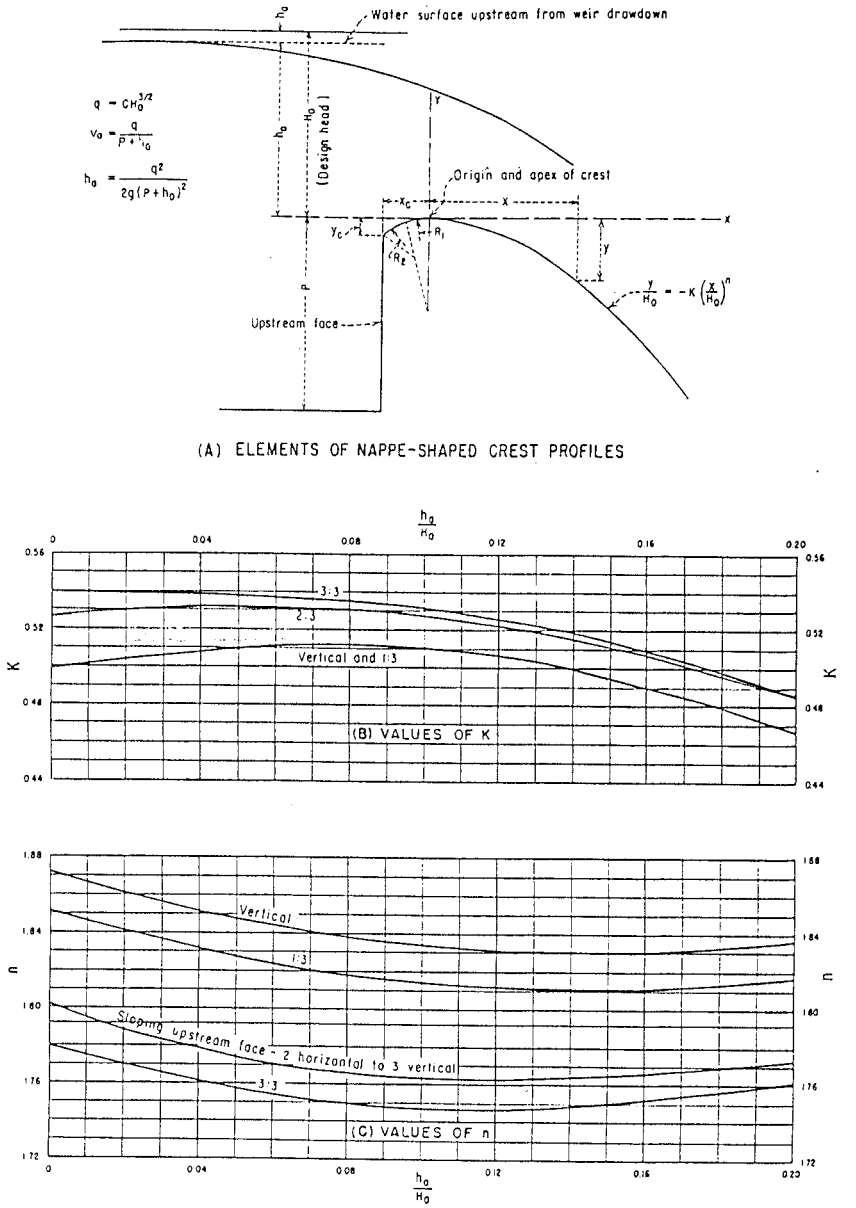

FIGURE 17.9 ***(a)*** Factors for the definition of nappe-shaped crest profiles (USBR, 1987)

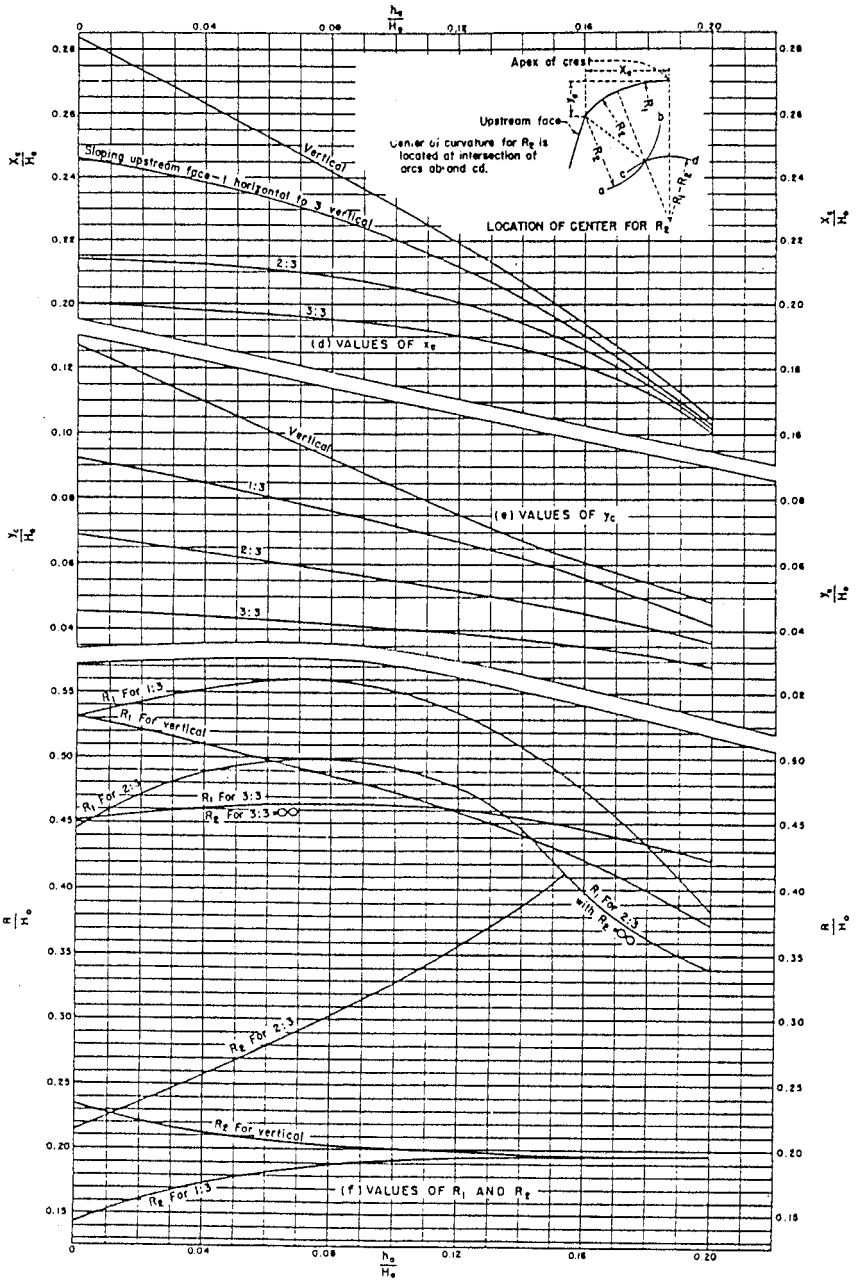

FIGURE 17.9(b) Factors (x_c, y_c, R_1, and R_2) for definition of nappe-shaped crest profiles.(USBR, 1987)

(a)

(b)

(c)

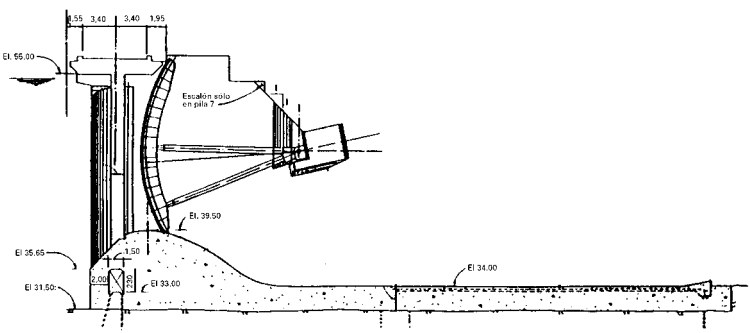

(d)

Exhibit 17.1 Macagua hydroelectric project, Venezuela (*Courtesy CVG–EDELCA, Caracas.*)
(a) General view of the spillway in operation.
(b) Free flow condition at the ogee crest.
(c) Flow condition at the ogee crest with gate partially open.
(d) Layout of the spillway and stilling basin.

(a)

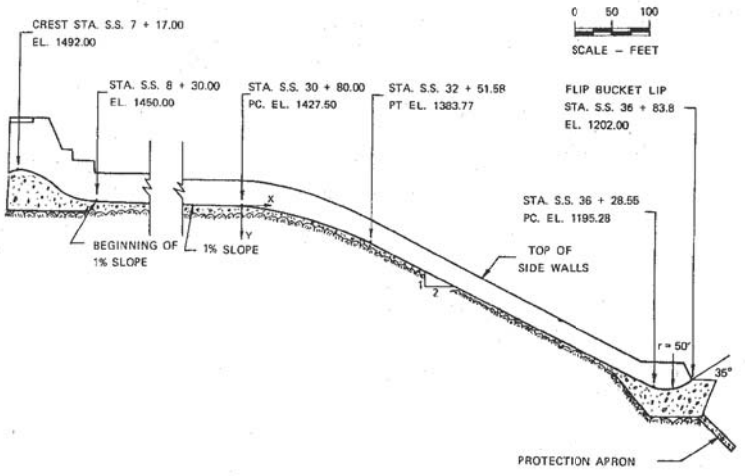

(b)

Exhibit 17.2 Tarbela hydroelectric project, Pakistan (*Courtesy water and power development authority, Pakistan*)
(a) General view of the spillway in operation.
(b) Layout of the spillway including the flip bucket.

17.3 OVERFALL SPILLWAY

An *overfall spillway* can be gated or ungated and provide for flow over an arch or arch-buttress dam, wherein the flow free-falls some distance before entering a plunge-pool energy dissipator in the tailrace. The hydraulic characteristics are defined as follows:

1. The crest structure and discharge rating are similar to those for the overflow spillway.
2. The flow normally leaves this structure shortly below the crest. The exit structure is normally some variation of a flip-bucket.
3. The flip-bucket radius for an overfall spillway is normally smaller than the ideal, which is at least $5d$, where d is the flow depth at the bottom of the bucket. The radius is usually undersized to minimize the size of the overhang, which can destabilize the top of a thin-arch dam. However, the radius should be sufficient to fully—deflect a significant flood say, the 100-year event.
4. The bucket exit angle is selected to throw the jet to a suitable location in the tailrace. The trajectory can be estimated by

$$y = x \tan \theta - \frac{x^2}{3.6H \cos^2\theta} \tag{17.3}$$

   where: y = vertical distance from the bucket lip x = horizontal distance from the buck et lip θ = bucket exit angle, and H = depth + velocity head at the bucket lip.
5. The trajectory can be estimated from Step 4 as long as the bucket radius exceeds $5d$. For larger depths, the flow overrides the bucket and will fall short of the maximum trajectory. The trajectory in this range is determined best by a physical model.
6. Pressure load on the bucket can be estimated from Fig. 17.10. For larger floods, where $d > R/5$, this load is determined best by a physical model.
7. The energy from an overfall spillway is normally dissipated by a plunge pool, which can be lined or unlined. If unlined, the scour and the scour rate will be based on both flow and geology. The scour hole development is usually indeterminate. However, the terminal scour depth for a uniformly erodible material can be esti-mated from the following empirical formula and from Fig. 17.11 (Coleman, 1982; USBR, 1987)

$$y_s = d_s \sin\alpha = \text{terminal vertical scour depth} \tag{17.4}$$

and

$$d_s = C_s H^{0.225} q^{0.54} \tag{17.5}$$

where C_s = 1.32 (for units in ft and cfs/ft) 1.90 (for units in m and cms/m), H = effective head at tailwater level, q = unit discharge = Q/B, B = width of the bucket, and α = average jet entry angle.

The extent of the scour hole is based on judgment of stable slope of material surrounding the deepest hole. A physical model is normally used where topography is complex and where scour can endanger project structures.

8. As the jet plunges into the pool, it diffuses almost linearly and entrains air at the surface of the pool and the water from the pool at the boundary of the jet. The behavior of the plunging jet, including dynamic pressures, can be approximated (Hinchliff and Houston, 1984) using Fig. 17.12 and Table 17.1 for both rectangular and circular jets.
9. If the plunge pool is lined because the scour would be unpredictable and unacceptable, the lining must be designed for pressure pulsations from the jet's impact. The design pressures can be determined best from physical model studies.

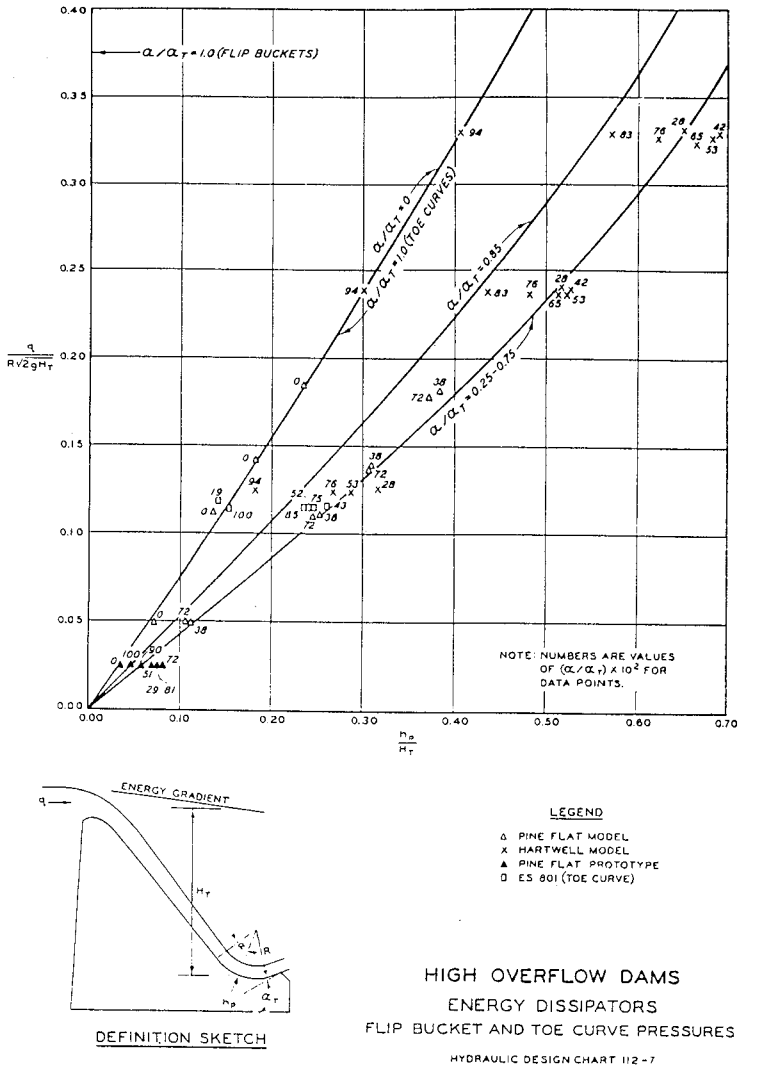

FIGURE 17.10 Pressures for flip-buckets and toe curves of an overflow spillway. (USACE, 1988).

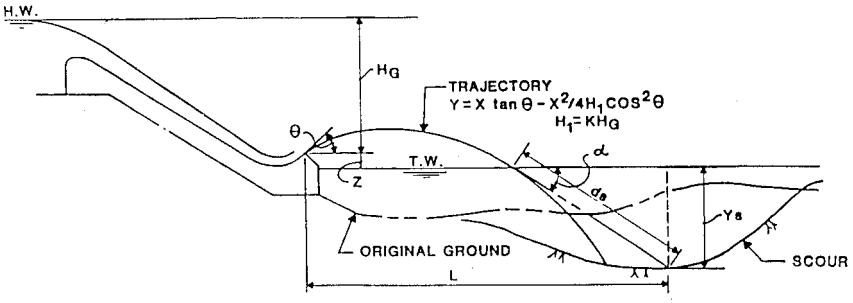

FIGURE 17.11 Definition sketch of free-jet trajectory and scour depth of an overflow spillway. (Coleman, 1982)

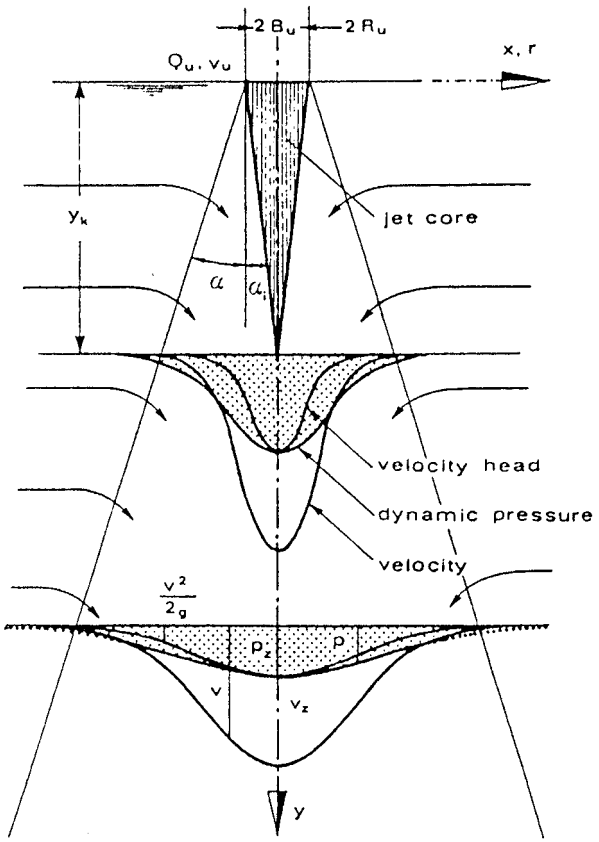

FIGURE 17.12 Schematic diagram of a diffusing plunging jet. (Vischer and Hager, 1995).

TABLE 17.1 Plunging Jet Characteristics (Whittaker and Schleiss, 1984)

		Rectangular jet	*Circular jet*
$y \le y_k$	$\frac{v_z}{v_u}$	1	1
	$\frac{p_z}{p_u}$	1	1
	$\frac{Q}{Q_u}$	$1 + 0.414\ y/y_k$	$1 + 0.507\ y/y_k + 0.500\ (y/y_k)^2$
	$\frac{E}{E_u}$	$1 - 0.184\ y/y_k$	$1 - 0.550\ y/y_k + 0.217(y/y_k)^2$
	$\frac{v}{v_z}$	$e^{-\pi/8(1\ +\ x/B_u \cdot y/y/y_k - y_k/y)^2}$	$e^{-1/2(1\ +\ r/R_u \cdot Y_k/y - y_k/y)^2}$
	$\frac{p}{p_z}$	$e^{-\pi/16(x/B_u)^2}$	$e^{-1/2(r/R_u)^2}$
$y \ge y_k$	$\frac{v_z}{v_u}$	$\sqrt{y_k/y}$	y_k/y
	$\frac{p_z}{p_u}$	y_k/y	$(y_k/y)^2$
	$\frac{Q}{Q_u}$	$1.414\ \sqrt{y/y_k}$	$2y/y_k$
	$\frac{e}{E_u}$	$0.816\ \sqrt{y/_k y}$	$0.667\ y_k/y$
	$\frac{v}{v_z}$	$e^{-\pi/8(x\backslash B_u \cdot y_k/y)^2}$	$e^{-1/2(r/R_u \cdot y_k/y)^2}$
	$\frac{p}{p_z}$	$e^{-\pi 16(x/B_u \cdot y_k/y)^2}$	$e^{-1/4(r/R_u \cdot y_k/y)^2}$

Source: Whittaker and Schleiss (1984).

(a)

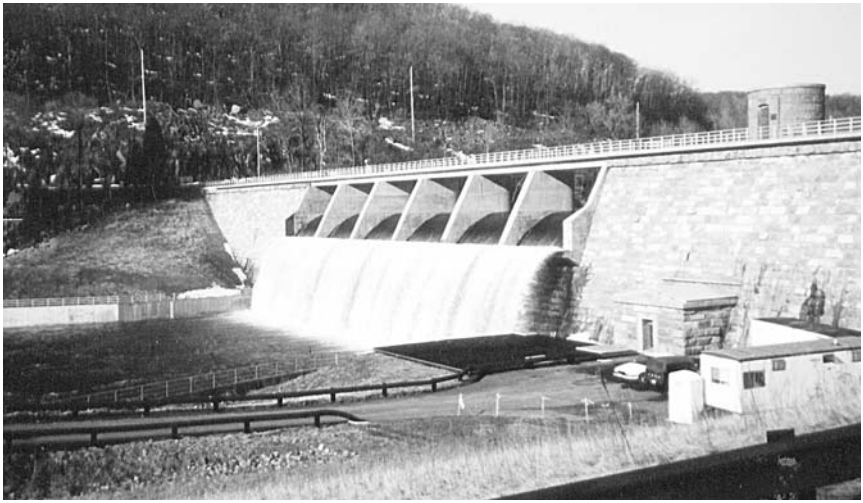

(b)

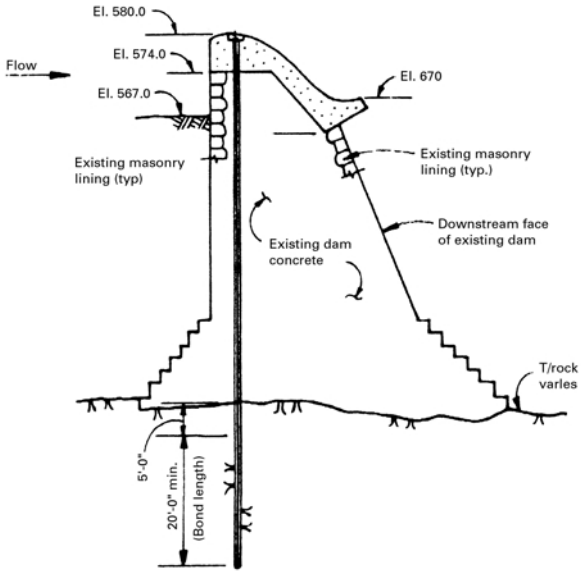

(c)

Exhibit 17.3 Boyd's corner dam project, New York.
(a) General view of the spillway
(b) A view of the overfall spillway in operation.
(c) Layout of the spillway including the flip bucket.

Exhibit 17.3 illustrates an overfall spilling in operation.

17.4 SIDE-CHANNEL SPILLWAY

A *side-channel spillway* can be gated or ungated and provides for flow into a chute or tunnel at right angles because the abutment topography is not favorable for a normal crest alignment. Figure 17.13 shows a typical arrangement. Exhibit 17.4 illustrates a side-channel spillway in operation The hydraulic features are defined as follows (USBR, 1987):

1. The crest is often ungated since a long crest may be suitable because of favorable topography.
2. The crest shape is based on the same criteria as the criteria for an overflow spillway.
3. The trough is sized by trial and error to prevent the maximum discharge water surface from encroaching on the crest's free-discharge capacity. The trough should be as nearly V-shaped as possible to maximize efficient dissipation of energy.
4. The chute crest is proportioned to produce subcritical flow in the trough for all discharges to dissipate the overflow energy and produce uniform flow into the chute.
5. The trough geometry for the first trial is proportioned to produce an approximately uniform reduction in trough velocity from downstream to upstream. This will usually minimize the trough size.
6. The water surface profile in the trough is estimated by the following:

$$\Delta Y = \frac{Q_2\,(V_1 + V_2)}{g\,(Q_1 + Q_2)}\left[(V_2 - V_1) + V_1\,\frac{(Q_2 - Q_1)}{Q_2}\right] \tag{17.6}$$

where ΔY = change in water level between two sections ΔX apart, Q_2, V_2 = discharge and velocity at the downstream section, and Q_1, V_1 = discharge and velocity at the upstream section. The computation begins with a known water level at the downstream end produced by critical depth control at the chute crest, and proceeds upstream in increments of ΔX by trial and error, calculating the water level along the length of the side channel. If the calculated water profile encroaches on the side channel's capacity, the geometry of the trough or chute crest or both should be adjusted.

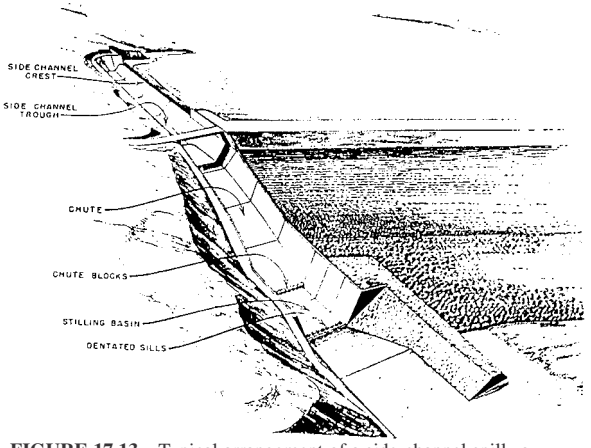

FIGURE 17.13 Typical arrangement of a side-channel spillway. (USBR, 1987).

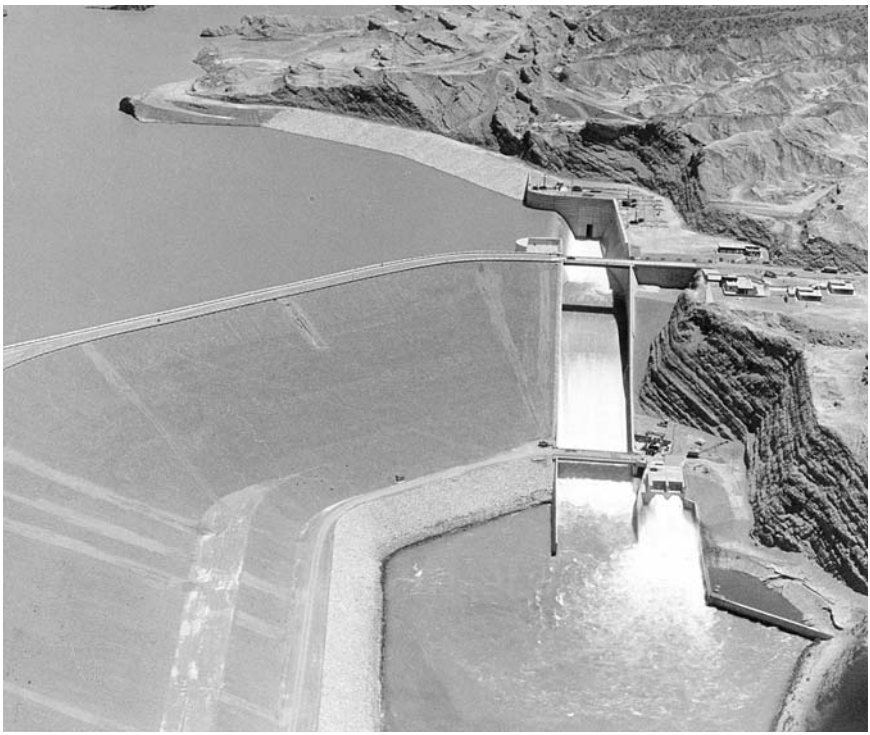

(a)

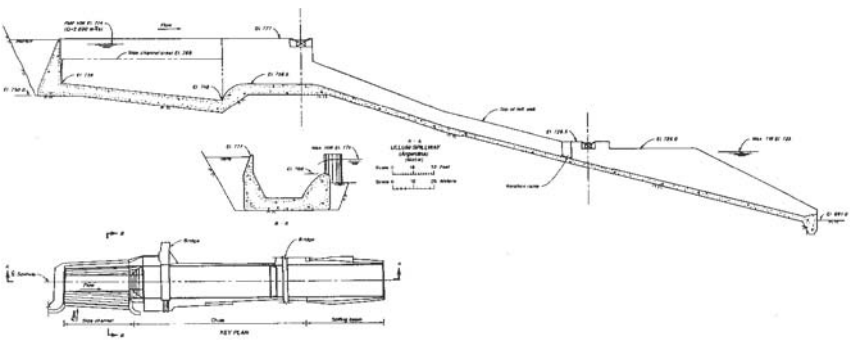

(b)

Exhibit 17.4 Ullum dam project, Argentina.
(a) General view of the side–channel spillway in operation
(b) Layout of the spillway including the stiling basin.

7. Once an acceptable geometry for the trough and chute crest has been determined, the chute should be sloped to provide supercritical flow away from the chute crest.
8. Large side-channel spillways are almost always model-tested because of the complex flow conditions in the trough area.

17.5 ORIFICE SPILLWAY

An *orifice spillway* is normally gated and is used when substantial discharge capacity is needed at low reservoir levels, as illustrated in Exhibit 17.5. For instance, it is useful when sediment sluicing is required. It also is useful for diverting flow during construction. Gate sizes are normally smaller for these spillways, but higher head and sealing details can make them expensive.

Orifice spillways can be found in gravity dams, adjacent to embankment dams, and in arch dams. Figs. 17.14 and 17.15 show a typical layout. The proportions of the orifice are defined as follows:

1. Gates are sized on the basis of discharge requirements at maximum and minimum headwater levels. The discharge coefficient can be assumed to be 0.90.
2. The roof curve must be shaped carefully to prevent cavitation if the head is high. For instance, the design in Fig. 17.15 has a roof curve composed of a circular curve with a large radius, followed by a 1:15 roof slope to the gates top seal. This shape was based on a physical model test (Fig. 17.14).

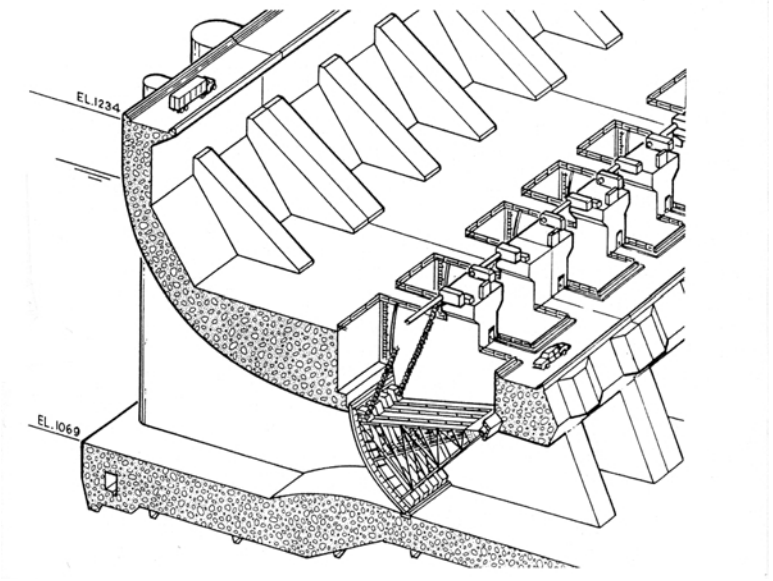

(a)

Exhibit 17.5 Mangla hidroelectric project, Paskistan A three–dimensional rendition of the spillway control structure.(*Courtesy Water and Power Development Authority, Pakistan).*

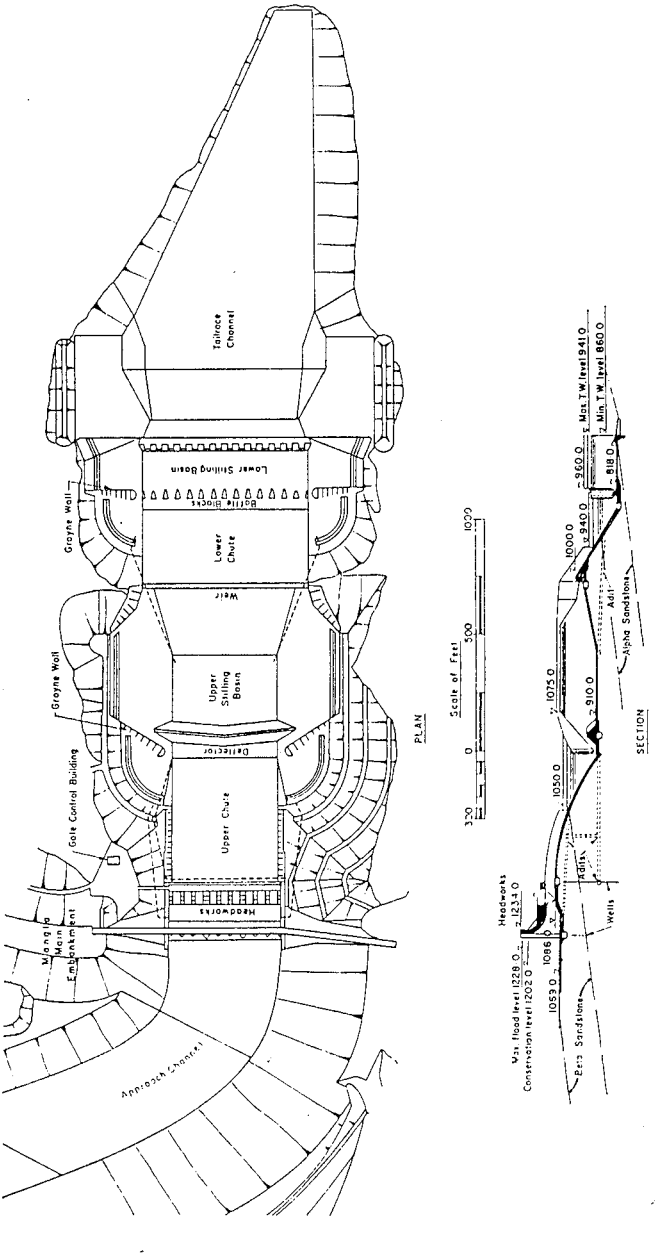

FIGURE 17.14 Typical arrangement of an orifice spillway. (Institute of Civil Engineers, (1968).

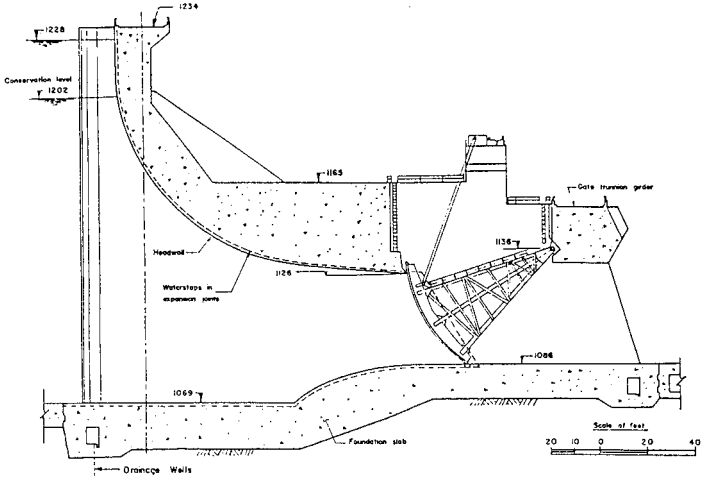

FIGURE 17.15 Typical arrangement of an orifice spillway control structure. (Institute of Civil Engineers, 1968)

3. The floor curve is less critical; however, for the design in Figs. 17.14 and 17.15 the curve radius was 150 ft.
4. Potential formation of vortex is a special concern for orifice spillways. A vortex suppressor will generally be required and can be determined by a physical model.
5. The spillway downstream of the gate structure changes to a chute that may lead to a stilling basin (see Figs. 17.14 and 17.15) or a flip-bucket.

17.6 MORNING GLORY SPILLWAY

The *morning glory spillway* is normally used in conjunction with a tunnel spillway when the intake is a vertical shaft. Also, because of flow entry from the entire periphery, the crest capacity is relatively high. Crest gates are not normally used because of access and cost considerations as well as poor hydraulic conditions in the shaft with partially open gates Exhibit 17.6 illustrates a morning glory spillway. Figures 17.16 and 17.17 show the range of possible flow conditions in the crest area for a morning-glory spillway (USBR,1987). The design procedure is as follows:

1. By trial and error, determine the required design head H_o and the crest radius from Fig. 17.18; $H_o/Rs = 0.3$ is recommended. Note that in Fig. 17.18, the discharge coefficient C_o is for English units. For metric units, the coefficient should be multiplied by a conversion factor of 0.552.
2. Determine the discharge rating curve for the full range of heads from Fig. 17.19.
3. Determine the lower nappe profile from Figs. 17.17 and 17.20 and Tables 17.2, 17.3, and 17.4.

4. Check for throat control in the shaft using the following:

$$R = C_R \frac{Q^{1/2}}{H_a^{1/4}} \tag{17.7}$$

where: $C_R = 0.275$ for units in m and m³/sec, $= 0.204$ for units in ft and ft³/sec, $R =$

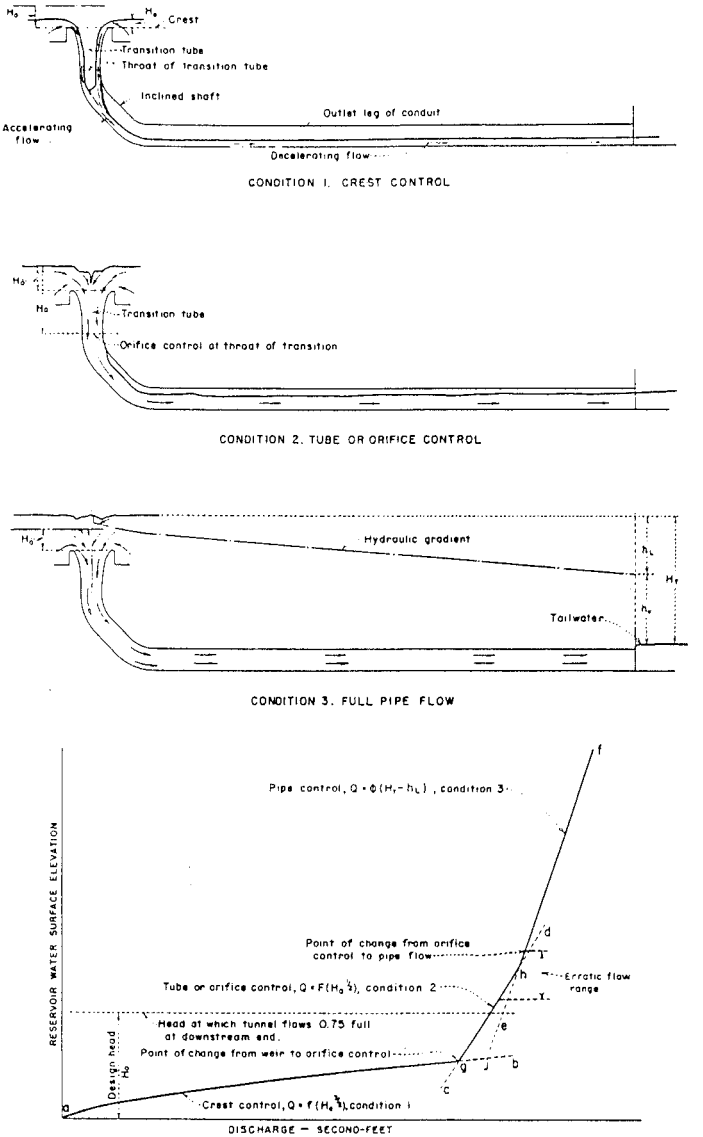

FIGURE 17.16 Possible flow conditions for a morning-glory spillway. (USBR, 1987).

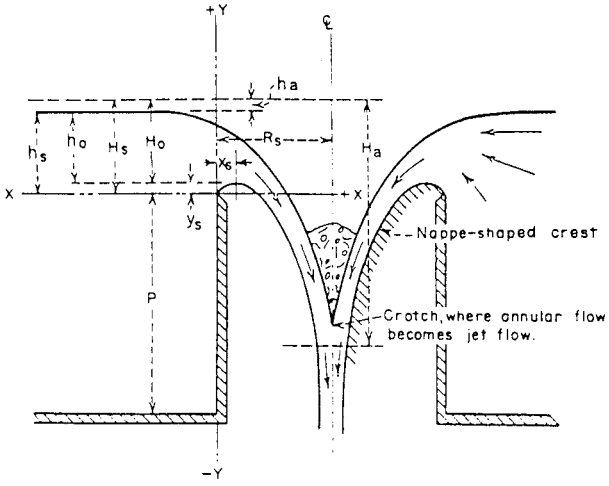

FIGURE 17.17 Elements of nappe-shaped profile for a morning-glory spillway. (USBR, 1987)

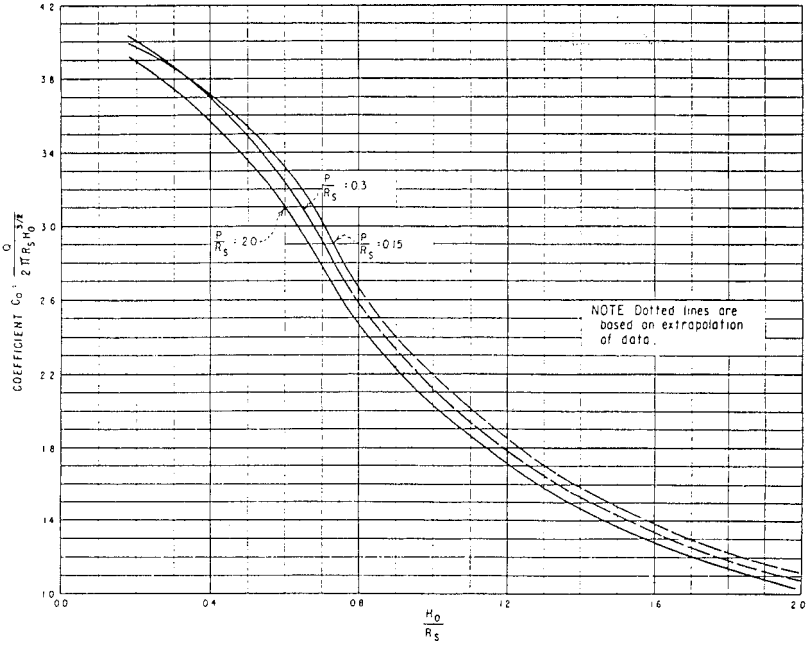

FIGURE 17.18 Circular crest coefficients for a morning-glory spillway with aerated nappe. (USBR, 1987)

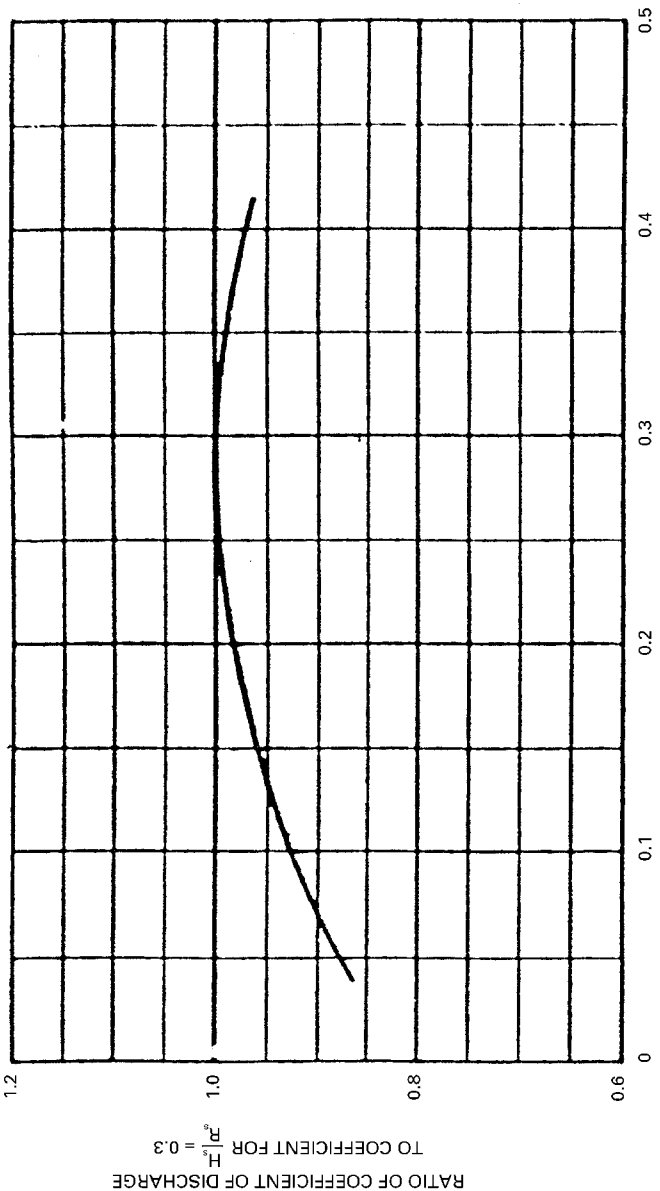

FIGURE 17.19 Circular crest coefficients of discharge for other than design head. (USBR, 1987)

TABLE 17.2 Coordinates of Lower Nappe Surface for Different Values of H_s/R When $P/R = 0.15$

$\frac{H_s}{R}$	0.20	0.2	0.30	0.35	0.40	0.45	0.50	0.60	0.80
$\frac{X}{H_s}$	$\frac{Y}{H_s}$ For portion of the profile above the weir crest								
0.000	0.0000	0.0000	0.0000	0.0000	0.0000	0.0000	0.0000	0.0000	0.0000
.010	.0120	.0120	.0115	.0115	.0110	.0110	.0105	.0100	.0090
.020	.0210	.0200	.0195	.0190	.0185	.0180	.0170	.0160	.0140
.030	.0285	.0270	.0265	.0260	.0250	.0235	.0225	.0200	.0165
.040	.0345	.0335	.0325	.0310	.0300	.0285	.0265	.0230	.0170
.050	.0405	.0385	.0375	.0360	.0345	.0320	.0300	.0250	.0170
.060	.0450	.0430	.0420	.0400	.0380	.0355	.0330	.0365	.0165
.070	.0495	.0470	.0455	.0430	.0410	.0380	.0350	.0270	.0150
.080	.0525	.0500	.0485	.0460	.0435	.0400	.0365	.0270	.0130
.090	.0560	.0530	.0510	.0480	.0455	.0420	.0370	.0265	.0100
.100	.0590	.0560	.0535	.0500	.0465	.0425	.0375	.0255	.0065
.120	.0630	.0600	.0570	.0520	.0480	.0435	.0365	.0220	
.140	.0660	.0620	.0585	.0525	.0475	.0425	.0345	.0175	
.160	.0670	.0635	.0590	.0520	.0460	.0400	.0305	.0110	
.180	.0675	.0635	.0580	.0500	.0435	.0365	.0260	.0040	
.200	.0670	.0625	.0560	.0465	.0395	.0320	.0200		
.250	.0615	.0560	.0470	.0360	.0265	.0160	.0015		
.300	.0520	.0440	.0330	.0210	.0100				
.350	.0380	.0285	.0165	.0030					
.400	.0210	.0090							
.450	.0015								
.500									
.550									
$\frac{Y}{H_s}$	$\frac{X}{H_s}$ For portion of the profile below the weir crest								
—0.000	0.454	0.422	0.392	0.358	0.325	0.288	0.253	0.189	0.116
—.020	.499	.467	.437	.404	.369	.330	.292	.228	.149
—.040	.540	.509	.478	.444	.407	.368	.328	.259	.174
—.060	.579	.547	.516	.482	.443	.402	.358	.286	.195
—.080	.615	.583	.550	.516	.476	.434	.386	.310	.213
—.100	.650	.616	.584	.547	.506	.462	.412	.331	.228
—.150	.726	.691	.660	.620	.577	.526	.468	.376	.263
—.200	.795	.760	.729	.685	.639	.580	.516	.413	.293
—.250	.862	.827	.790	.743	.692	.627	.557	.445	.319
—.300	.922	.883	.843	.797	.741	.671	.594	.474	.342
—.400	1.029	.988	.947	.893	.828	.749	.656	.523	.381
—.500	1.128	1.086	1.040	.980	.902	.816	.710	.567	.413
—.600	1.220	1.177	1.129	1.061	.967	.869	.753	.601	.439
—.800	1.380	1.337	1.285	1.202	1.080	.953	.827	.655	.473
—1.000	1.525	1.481	1.420	1.317	1.164	1.014	.878	.696	.498
—1.200	1.659	1.610	1.537	1.411	1.228	1.059	.917	.725	.517
—1.400	1.780	1.731	1.639	1.480	1.276	1.096	.949	.750	.531
—1.600	1.897	1.843	1.729	1.533	1.316	1.123	.973	.770	.544
—1.800	2.003	1.947	1.809	1.580	1.347	1.147	.997	.787	.553
—2.000	2.104	2.042	1.879	1.619	1.372	1.167	1.013	.801	.560
—2.500	2.340	2.251	2.017	1.690	1.423	1.210	1.049	.827	
—3.000	2.550	2.414	2.105	1.738	1.457	1.240	1.073	.840	
—3.500	2.740	2.530	2.153	1.768	1.475	1.252	1.088		
—4.000	2.904	2.609	2.180	1.780	1.487	1.263			
—4.500	3.048	2.671	2.198	1.790	1.491				
—5.000	3.169	2.727	2.207	1.793					
—5.500	3.286	2.769	2.210						
—6.000	3.396	2.800							
$\frac{Hs}{R}$	0.20	0.25	0.30	0.35	0.40	0.45	0.50	0.60	0.80

Source: USBR (1987).

TABLE 17.3 Coordinates of Lower Nappe Surface for Different Values of H_s/R When $P/R = 0.30$

$\frac{H_s}{R}$	0.20	0.2	0.30	0.35	0.40	0.45	0.50	0.60	0.80
$\frac{X}{H_s}$	$\frac{Y}{H_s}$ For portion of the profile above the weir crest								
0.000	0.0000	0.0000	0.0000	0.0000	0.0000	0.0000	0.0000	0.0000	0.0000
.010	.0130	.0130	.0130	.0125	.0120	.0120	.0115	.0110	.0100
.020	.0245	.0242	.0240	.0235	.0225	.0210	.0195	.0180	.0170
.030	.0340	.0335	.0330	.0320	.0300	.0290	.0270	.0240	.0210
.040	.0415	.0411	.0390	.0380	.0365	.0350	.0320	.0285	.0240
.050	.0495	.0470	.0455	.0440	.0420	.0395	.0370	.0325	.0245
.060	.0560	.0530	.0505	.0490	.0460	.0440	.0405	.0350	.0250
.070	.0610	.0575	.0550	.0530	.0500	.0470	.0440	.0370	.0245
.080	.0660	.0620	.0590	.0565	.0530	.0500	.0460	.0385	.0235
.090	.0705	.0660	.0625	.0595	.0550	.0520	.0480	.0390	.0215
.100	.0740	.0690	.0660	.0620	.0575	.0540	.0500	.0395	.0190
.120	.0800	.0750	.0705	.0650	.0600	.0560	.0510	.0380	0.120
.140	.0840	.0790	.0735	.0670	.0615	.0560	.0515	.0355	.0020
.160	.0870	.0810	.0750	.0675	.0610	.0550	.0500	.0310	
.180	.0885	.0820	.0755	.0675	.0600	.0535	.0475	.0250	
.200	.0885	.0820	.0745	.0660	.0575	.0505	.0435	.0.180	
.250	.0855	.0765	.0685	.0590	.0480	.0390	.0270		
.300	.0780	.0670	.0580	.0460	.0340	0.220	.0050		
.350	.0660	.0540	.0425	.0295	.0150				
.400	.0495	.0370	.0240	.0100					
.450	.0300	.0170	.0025						
.500	.0090	—.0060							
.550									
$\frac{Y}{H_s}$	$\frac{X}{H_s}$ For portion of the profile below the weir crest								
—0.000	0.519	0.488	0.455	0.422	0.384	0.349	0.310	0.238	0.144
—.020	.560	.528	.495	.462	.423	.387	.345	.272	.174
—.040	.598	.566	.532	.498	.458	.420	.376	.300	.198
—.060	.632	.601	.567	.532	.491	.451	.406	.324	.220
—.080	.664	.634	.600	.564	.522	.480	.432	.348	.238
—.100	.693	.664	.631	.594	.552	.508	.456	.368	.254
—.150	.760	.734	.701	.661	.618	.569	.510	.412	.290
—.200	.831	.799	.763	.723	.677	.622	.558	.451	.317
—.250	.893	.860	.826	.781	.729	.667	.599	.483	.341
—.300	.953	.918	.880	.832	.779	.708	.634	.510	.362
—.400	1.060	1.024	.981	.932	.867	.780	.692	.556	.396
—.500	1.156	1.119	1.072	1.020	.938	.841	.745	.595	.424
—.600	1.242	1.203	1.153	1.098	1.000	.891	.780	.627	.446
—.800	1.403	1.359	1.301	1.227	1.101	.970	.845	.672	.478
—1.000	1.549	1.498	1.430	1.333	1.180	1.028	.892	.707	.504
—1.200	1.680	1.622	1.543	1.419	1.240	1.070	.930	.733	.521
—1.400	1.800	1.739	1.647	1.489	1.287	1.106	.959	.757	.540
—1.600	1.912	1.849	1.740	1.546	1.323	1.131	.983	.778	.551
—1.800	2.018	1.951	1.821	1.590	1.353	1.155	1.005	.797	.560
—2.000	2.120	2.049	1.892	1.627	1.380	1.175	1.022	.810	.569
—2.500	2.351	2.261	2.027	1.697	1.428	1.218	1.059	.837	
—3.000	2.557	2.423	2.113	1.747	1.464	1.247	1.081	.852	
—3.500	2.748	2.536	2.167	1.778	1.489	1.263	1.099		
—4.000	2.911	2.617	2.200	1.796	1.499	1.274			
—4.500	3.052	2.677	2.217	1.805	1.507				
—5.000	3.173	2.731	2.223	1.810					
—5.500	3.290	2.773	2.228						
—6.000	3.400	2.808							
$\frac{Hs}{R}$	0.20	0.25	0.30	0.35	0.40	0.45	0.50	0.60	0.80

Source: USBR (1987).

TABLE 17.4 Coordinates of Lower Nappe Surface for Different Values of H_s/R When $P/R = 2.00$

$\frac{H_s}{R}$	0.00	0.10*	0.20	0.25	0.30	0.35	0.40	0.45	0.50	0.60	0.80	1.00	1.20	1.50	2.00
$\frac{X}{H_s}$	$\frac{Y}{H_s}$ For portion of the profile above the weir crest														
0.000	0.0000	0.0000	0.0000	0.0000	0.0000	0.0000	0.0000	0.0000	0.0000	0.0000	0.0000	0.0000	0.0000	0.0000	0.0000
.010	.0150	.0145	.0133	.0130	.0128	.0125	.0122	.0119	.0116	.0112	.0104	.0095	.0086	.0077	.0070
.020	.0280	.0265	.0250	.0243	.0236	.0231	.0225	.0220	.0213	.0202	.0180	.0159	.0140	.0115	.0090
.030	.0395	.0365	.0350	.0337	.0327	.0317	.0308	.0299	.0289	.0270	.0231	.0198	.0168	.0126	.0085
.040	.0490	.0460	.0435	.0417	.0403	.0389	.0377	.0363	.0351	.0324	.0268	.0220	.0176	.0117	.0050
.050	.0575	.0535	.0506	.0487	.0471	.0454	.0436	.0420	.0402	.0368	.0292	.0226	.0168	.0092	
.060	.0650	.0605	.0570	.0550	.0531	.0510	.0489	.0470	.0448	.0404	.0305	.0220	.0147	.0053	
.070	.0710	.0665	.0627	.0605	.0584	.0560	.0537	.0514	.0487	.0432	.0308	.0201	.0114	.0001	
.080	.0765	.0710	.0677	.0655	.0630	.0603	.0578	.0550	.0521	.0455	.0301	.0172	.0070		
.090	.0820	.0765	.0722	.0696	.0670	.0640	.0613	.0581	.0549	.0471	.0287	.0135	.0018		
.100	.0860	.0180	0.762	.0734	.0705	.0672	.0642	.0606	.0570	.0482	.0264	.0089			
.120	.0940	.0880	.0826	.0790	.0758	.0720	.0683	.0640	.0596	.0483	.0195				
.140	.1000	.0935	.0872	.0829	.0792	.0750	.0005	.0654	.0599	.0460	.0101				
.160	.1045	.0980	.0905	.0855	.0812	.0760	.0710	.0651	.0585	.0418					
.180	.1080	.1010	.0927	.0872	.0820	.0766	.0705	.0637	.0559	.0361					
.200	.1105	.1025	.0938	.0877	.0819	.0756	.0688	.0611	.0521	.0292					
.250	.1120	.1035	.0926	.0850	.0773	.0683	.0596	.0495	.0380	.0068					
.300	.1105	.1000	.0850	.0764	.0668	.0559	.0446	.0327	.0174						
.350	.1060	.0930	.0750	.0650	.0540	.0410	.0280	.0125							
.400	.0970	.0830	.0620	.0500	.0365	.0220	.0060								
.450	.0845	.0700	.0450	.0310	.0170	.000									
.500	.0700	.0520	.0250	.0100											
.550	.0520	.0320	.0020												
.600	.0320	.0080													
.650	.0000														
$\frac{X}{H_s}$	$\frac{Y}{H_s}$ For portion of the profile below the weir crest														
0.000	0.668	0.615	0.554	0.520	0.487	0.450	0.413	0.376	0.334	0.262	0.158	0.116	0.093	0.070	0.048
–.020	.705	.652	.592	.560	.526	.488	.452	.414	.369	.293	.185	.145	.120	.096	.074
–.040	.742	.688	.627	.596	.563	.524	.487	.448	.400	.320	.212	.165	.140	.115	.088
–.0.60	.777	.720	.660	.630	.596	.557	.519	.478	.428	.342	.232	.182	.155	.129	.100
–.080	.808	.752	.692	.662	.628	.589	.549	.506	.454	.363	.250	.197	.169	.140	.110
–.100	.838	.784	.722	.692	.657	.618	.577	.532	.478	.381	.266	.210	.180	.150	.188
–.150	.913	.857	.793	.762	.725	.686	.641	.589	.531	.423	.299	.238	.204	.170	.132
–.200	.978	.925	.860	.826	.790	.745	.698	.640	.575	.459	.326	.260	.224	.184	.144
–.250	1.040	.985	.919	.883	.847	.801	.750	.683	.613	.490	.348	.280	.239	.196	.153
–.300	1.100	1.043	.976	.941	.900	.852	.797	.722	.648	.518	.368	.296	.251	.206	.160
–.400	1.207	1.150	1.079	1.041	1.000	.944	.880	.791	.706	.562	.400	.322	.271	.220	.168
–.500	1.308	1.246	1.172	1.131	1.087	1.027	.951	.849	.753	.598	.427	.342	.287	.232	.173
–.600	1.397	1.335	1.260	1.215	1.167	1.102	1.012	.898	.793	.627	.449	.359	.300	.240	.179
–.800	1.563	1.500	1.422	1.369	1.312	1.231	1.112	.974	.854	.673	.482	.384	.320	.253	.184
–.1.000	1.713	1.646	1.564	1.508	1.440	1.337	1.189	1.030	.899	.710	.508	.402	.332	.260	.188
–.1.200	1.846	1.780	1.691	1.635	1.553	1.422	1.248	1.074	.933	.739	.528	.417	.340	.266	
–.1.400	1.970	1.903	1.808	1.748	1.653	1.492	1.293	1.108	.963	.760	.542	.423	.344		
–.1.600	2.085	2.020	1.918	1.855	1.742	1.548	1.330	1.133	.988	.780	.553	.430			
–.1.800	2.196	2.130	2.024	1.957	1.821	1.591	1.358	1.158	1.008	.797	.563	.433			
–.2.000	2.302	2.234	2.126	2.053	1.891	1.630	1.381	1.180	1.025	.810	.572				
–.2.500	2.557	2.475	2.354	2.266	2.027	1.701	1.430	1.221	1.059	.838	.588				
–.3.000	2.778	2.700	2.559	2.428	2.119	1.748	1.468	1.252	1.086	.853					
–.3.500		2.916	2.749	2.541	2.171	1.777	1.489	1.267	1.102						
–.4.000		3.114	2.914	2.620	2.201	1.796	1.500	1.280							
–.4.500		3.306	3.053	2.682	2.220	1.806	1.509								
–.5.000		3.488	3.178	2.734	2.227	1.811									
–.5.500		3.653	3.294	2.779	2.229										
–.6.000		3.820	3.405	2.812	2.232										
$\frac{H}{R}$	0.00	0.10	0.20	0.25	0.30	0.35	0.40	0.45	0.50	0.60	0.80	1.00	1.20	1.50	2.00

•The tabulation for $\frac{H_s}{R} = 0.10$ was obtained by interpolation between $\frac{H_s}{R} = 0$ and 0.20.

Source: USBR (1987).

(a)

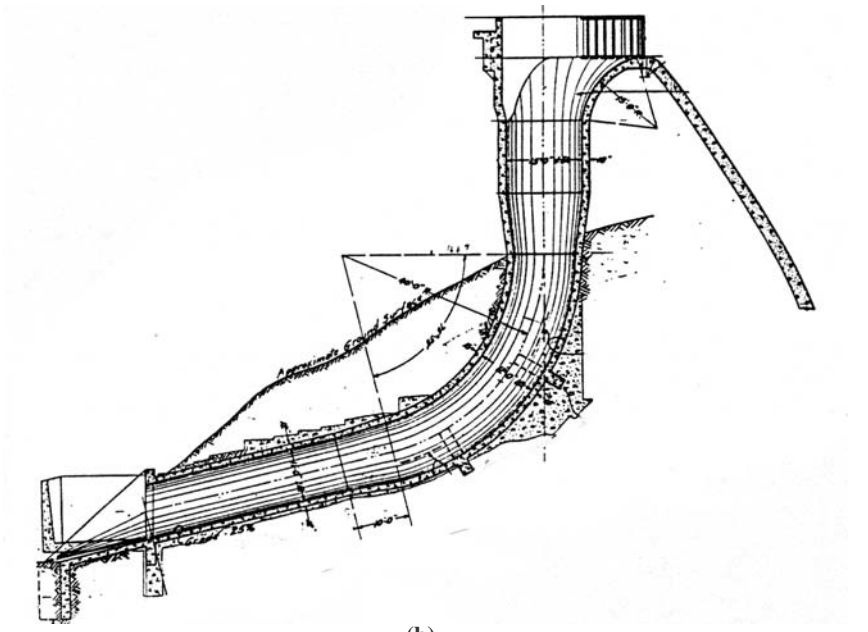

(b)

Exhibit 17.6 Big Dalton Dam, California
(a) General view of the modified morning–glory spillway.
(b) Layout of the spillway.

required shaft radius for throat control (m or ft), H_a = head from headwater level to throat location (m or ft), and Q = discharge under consideration (m^3/sec or ft^3/sec). If R exceeds the radius of the shaft for a given flow, then throat control exists and the discharge is based on the shaft radius.

5. The downstream tunnel is ordinarily sized to flow no more than three-fourths full with the maximum value of Manning's roughness coefficient $n = 0.016$ to avoid potentially unstable flow conditions. If the tunnel flows full, with throat control already developed, the capacity is dictated by full flow throughout.
6. An ideal design has crest control throughout the range of discharge.

17.7 LABYRINTH SPILLWAY

The *labyrinth spillway* is used to concentrate discharge into a narrow chute, where space does not permit a linear ungated crest. It generally minimizes approach excavation, whereas the concrete weir is more complicated to construct. Labyrinth spillways have been built with a wide range of sizes and discharge capacities and are well suited for rehabilitation of existing spillway structures when increased spillway capacity is needed (Hinchliff and Houston, 1984; Tacail et al., 1990; Tullis el al., 1995). Labyrinth structures can be built economically if an adequate foundation is available.

Figure 17.21 is a typical layout (Tacail et al., 1990). The most efficient spillway entrance for most reservoir applications is a curved approach adjacent to each end cycle of the spillway, with the approach flow parallel to the centerline of the spillway cycles for more uniform approach flow. The spillway entrance should be placed as far upstream in the reservoir as possible to reduce localized upstream head losses. To avoid the submergence effect, the supercritical flow condition should be maintained at the chute crest downstream from the labyrinth. The number of spillway cycles should be determined on the basis of the magnitude of the upstream head, the effect of nappe interference, and the economics of the design. With normal operating conditions, the vertical aspect ratio for each labyrinth cycle, w/P (Fig. 17.22), should be 2.5 or greater (Tullis et al., 1995).

Subatmospheric pressures under the nappe will cause nappe oscillation and noise and should be avoided by venting for structural reasons. Splitter piers can be placed along the spillway's side walls, or crushed stone can be placed along the downstream edge of the crest. The piers should be located at a distance equal to 8 to 10 percent of the wall length upstream of the downstream apexes (Tullis et al., 1995). Although the use of crushed stone may reduce the spillway's capacity, it can be cost effective. Discharge capacity is a function of the head over the crest, the height of the crest wall, the shape of the crest, the angle of the labyrinth, the number of cycles, and the length of the side leg (Tullis et al., 1995). An efficient design will result from the following procedure:

1. Knowing the design discharge and the maximum head, determine the required effective length from

$$Q = \frac{2}{3} C_d L \sqrt{2g} H_t^{3/2} \tag{17.8}$$

where $C_d = 0.30$ is derived from Fig. 17.23, with $\alpha = 8°$, and $H_t/p = 0.8$.

2. Fixing the apex A, determine the number of cycles in the labyrinth N from

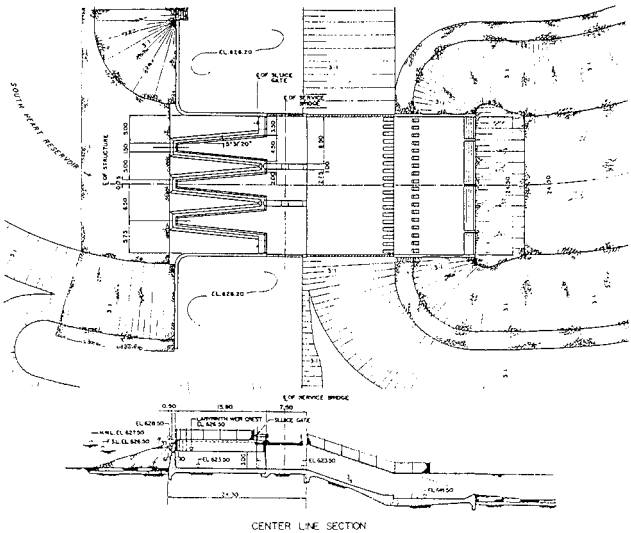

FIGURE 17.21 Layout of a typical labyrinth spillway. (Tacail et al., 1990).

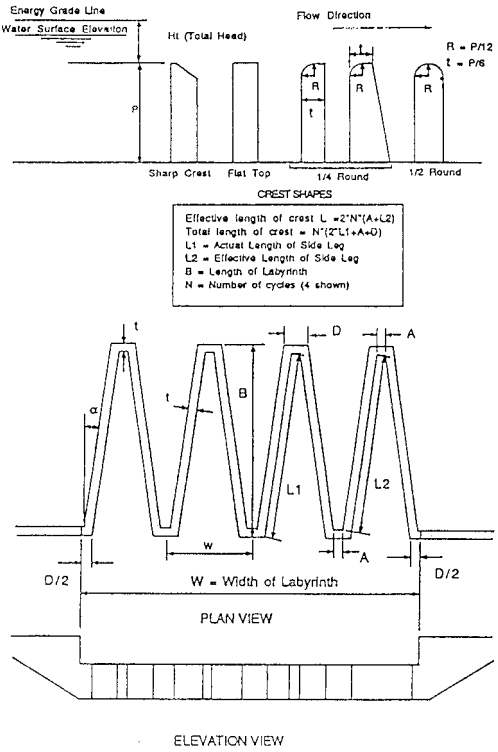

FIGURE 17.22 Layout and details of a labyrinth weir. (Tullis et al., 1995).

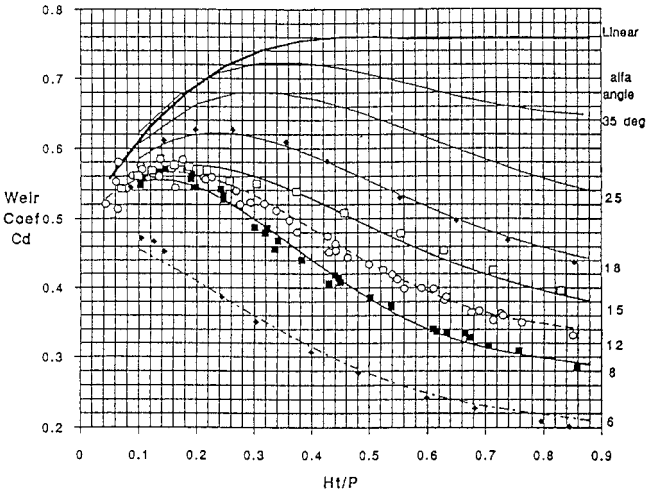

FIGURE 17.23 Crest discharge coefficient for labyrinth spillways. (Tullis et al., 1995).

$$L = 2N\,(A + L2) \tag{17.9}$$

where $L2$ is sized to produce an integral number N.

3. If the economics of labyrinth size must be confirmed, other trial sizes can be determined by assuming angles α other than 8° or by varying H_t/p (≤ 0.9) and repeating Steps 1 and 2. The costs of the approach channel and spillway chute, including the dissipator, may influence the ultimate selection of labyrinth geometry.
4. After selecting the labyrinth size, detail as follows: $t = P/6$, $R = P/12$, and $A = 1$ to 2 t. The crest shape is quarter-round.
5. The width of the spillway chute downstream is equal to W, the width of the labyrinth.
6. The chute slope must be supercritical for the entire flow range.

17.8 SIPHON SPILLWAY

17.8.1 Standard Siphon Spillway

A *standard siphon spillway* is used when a large discharge capacity is required in an extremely narrow head range without the use of operating gates. It is ideal for emergency overflows in remote locations. The type used most commonly is the standard or *blackwater* siphon, where there is a definite priming point, after which there is no air in the flow. Figures 17.24 and 17.25 show the design details for this spillway (USBR, 1987). To minimize losses, the upper leg transition should be well proportioned to provide gradually contracting area, and the inlet area should be about two or three times the area of the throat. The recommended design procedure is as follows:

1. Set the crest elevation.
2. Determine head available ($H_t \leq$ local atmospheric head).
3. Estimate number of siphon barrels required.
4. Determine d, B, D, and R_c, knowing the Q/barrel required, so that

$$Q/barrel = CBD\sqrt{2gH_t} \tag{17.10}$$

where d = depth of water at outlet, D = throat width, B = width of the rectangular siphon = $2D$ (recommended), C = discharge coefficient based on d/D and R_{CL} (Fig. 17.25), R_{CL} = radius of center-line of throat, and R_c = radius of crest of throat = R_{CL}-D/2.

Recommended ratio of R_{CL} to D is 2.5 for the throat at the upper and lower bends.

5. Check the theoretical limiting Q/barrel from

$$Q/barrel = BR_c\sqrt{0.7(2gh_{at})}\ \ln(R_s/R_c) \tag{17.11}$$

where R_s = the radius of curvature at the summit of the throat and h_{at} = local atmospheric head.

6. Adjust R_c (and D, if necessary) if the Q/barrel from Step 5 is less than from Step 4, until the result from Step 5 is ≥ than the result from Step 4.
7. Select the priming head on the basis of the desired operating level of the reservoir. If the priming head is less than D/2, locate P.C. of the lower bend on the trajectory of the nappe.
8. Determine the size and the inlet elevation of the siphon breaker (area of breaker = area of throat/24).
9. Select and design the priming aids to be used (slot to aerate the nappe, vent to equalize pressure above and below the nappe, and vent at the lower bend).

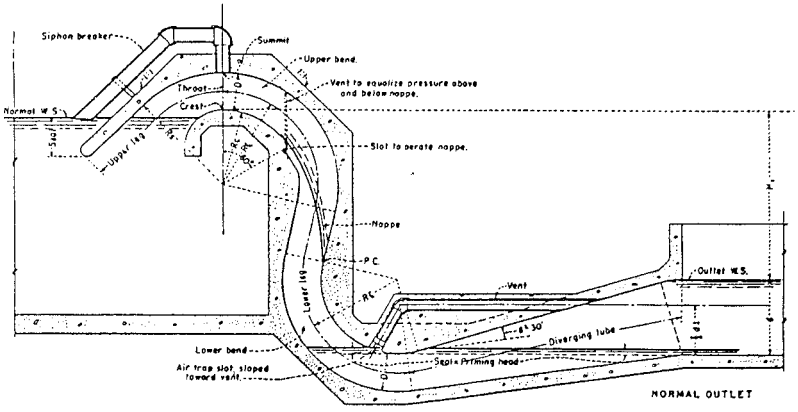

FIGURE 17.24 Typical standard siphon spillway. (USBR, 1987).

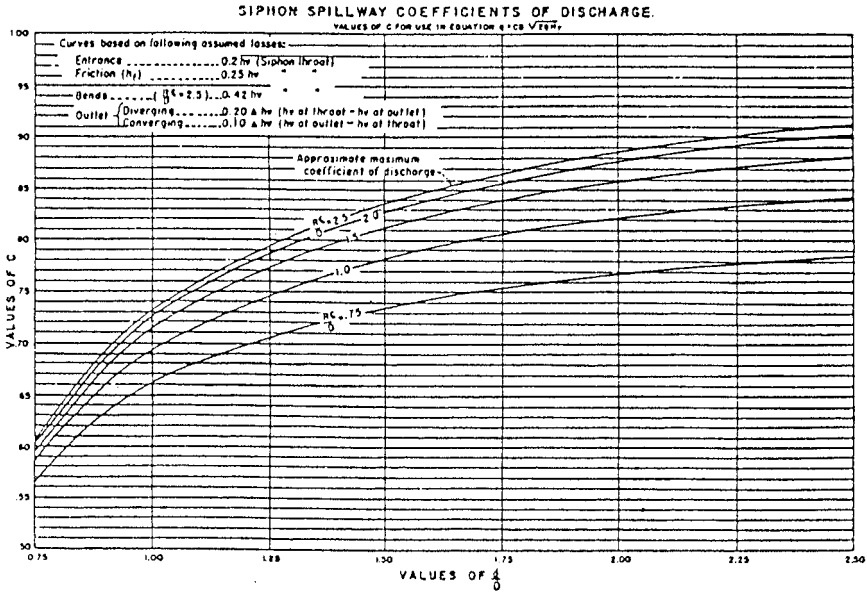

FIGURE 17.25 Discharge coefficients for standard siphon spillways. (USBR, 1987).

10. Set the upper bend-aeration slot at 60° from the vertical axis of the crest. Set the pipe vent in the sidewalls and connect the slot to the summit area.
11. Set the lower bend P.C. on the trajectory of nappe according to the priming head at the crest. Set the top of the vertical sections of the siphons lower bend at the elevation of the outlet bottom.
12. Set the elevation of the lower bend air trap at the elevation of the outlet bottom plus the priming head. Set the vent area = throat area / 48 (approximate).
13. Set the length of the diverging tube using an 8°30' angle of divergence, and set the vent outlet at two-thirds the depth of the outlet at maximum capacity.
14. Set the pipe vent of the siphon breaker at the summit, with the inlet end set at or slightly below the normal level of the reservoir. Set the minimum pipe area = throat area/24.
15. Set the submerged lip of the upper leg deep enough to provide good seal and to prevent excessive drawdown.

17.8.2 Air-Regulated Siphon Spillway

A disadvantage of the standard (nonaerated blackwater) siphon is the sudden increase in discharge on priming and the potential for "hunting" when the inflow is between priming flow

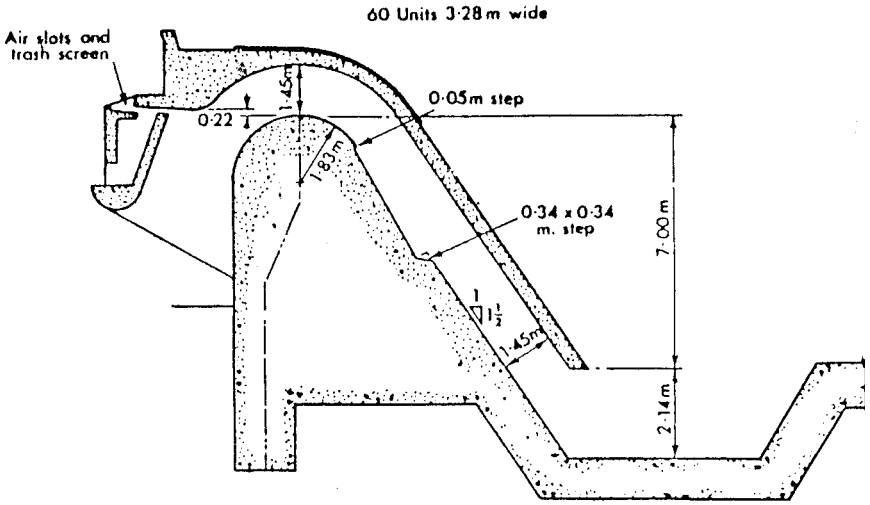

FIGURE 17.26 Typical air-regulated siphon spillway. (Ackers and Thomas, 1975).

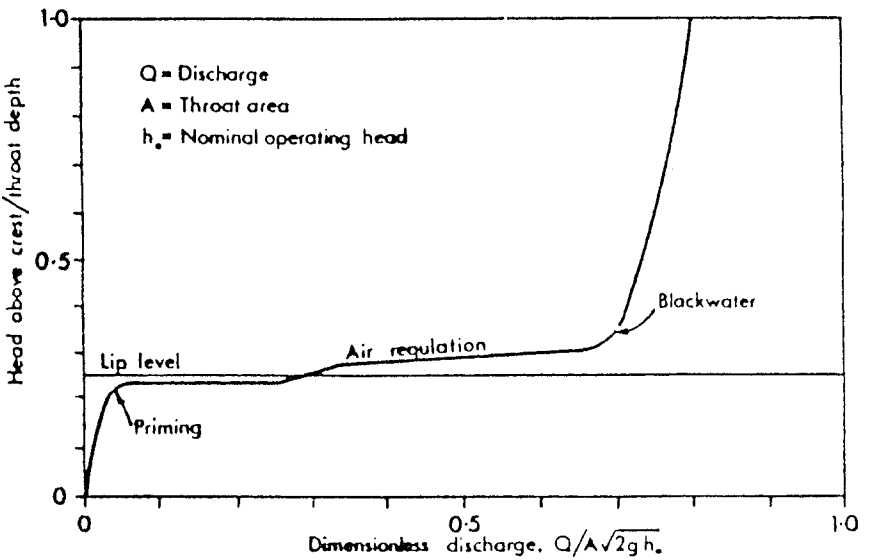

FIGURE 17.27 Typical discharge rating curve for air-regulated siphon spillways. (Ackers and Thomas, 1975)

and the siphon's capacity. An alternative called an *air-regulated* siphon is designed to operate in a steady-state condition for any discharge between priming and capacity and flowing full of a water-air mixture without reaching the blackwater condition. Therefore, it produces a more stable flow condition with a smoother transition during priming. This type of siphon was developed more than 50 years ago and has been used extensively in the Far East to pass floods of up to 2200 m^3/s (Ackers and Thomas, 1975). Its performance can be affected by waves, floating debris, and ice. Recent designs have provided corrections for these problems: for example, by installing of a vertical baffle wall at the upstream face of the siphon.

Figure 17.26 shows a typical layout, and Fig. 17.27 shows a typical discharge rating curve. Except for the air intake, the design of an air-regulated siphon spillway is generally similar to that of a standard siphon spillway. A preliminary design can be developed by scaling from a design that has been model tested (e.g., Fig. 17.26). However, because approach and exit flow conditions vary from project to project, each design should always be confirmed by model tests. In particular, the mixed-flow conditions, along with potential cavitation at the siphon crest (as with the standard siphon), make this design more complicated than the standard siphon. However, this design is preferable when flow conditions are highly variable. A summary of experience with air-regulated siphons is available in Ackers and Thomas (1975).

17.9 TUNNEL SPILLWAY

Tunnel spillways are used with embankment dams, where there is no suitable location for a chute spillway. A competent rock abutment is required. Tunnel spillways can be gated or ungated, depending on topographic and geologic constraints at the tunnel entrance. In some cases, gates may be required, as shown in Fig. 17.28. A tunnel spillway generally consists of the following elements: entrance structure, inclined tunnel section, flat tunnel section, and flip-bucket.

17.9.1 Entrance Structure

The *entrance structure* serves to provide the required discharge capacity and to transition the flow to the inclined tunnel section. If the entrance structure is ungated, it generally will be a side-channel crest with a trough designed in accordance with Sec. 17.4. If the entrance is gated, it may be by ogee crest gates or by orifice gates. If ogee crest gates are used, the ogee is shaped in accordance with Sec. 17.2, Step 9. If the entrance is a gated orifice, use Sec. 17.5.

The transition from an entrance structure to an inclined shaft must be gradual to maintain accelerating, supercritical, open-channel flow. The transition is usually from a rectangular section to a circular tunnel section. Angles of convergence should not exceed approximately 3° (1:20).

17.9.2 Inclined Tunnel Section

The *inclined tunnel* provides for acceleration of the flow from the entrance transition to the flat-tunnel section downstream. The inclined shaft is connected to the flat tunnel by a vertical curve with a large radius ($R/D \geq 5$). The elevation of the bottom of the curve should provide velocity and depth to satisfy the following energy consistent with head-

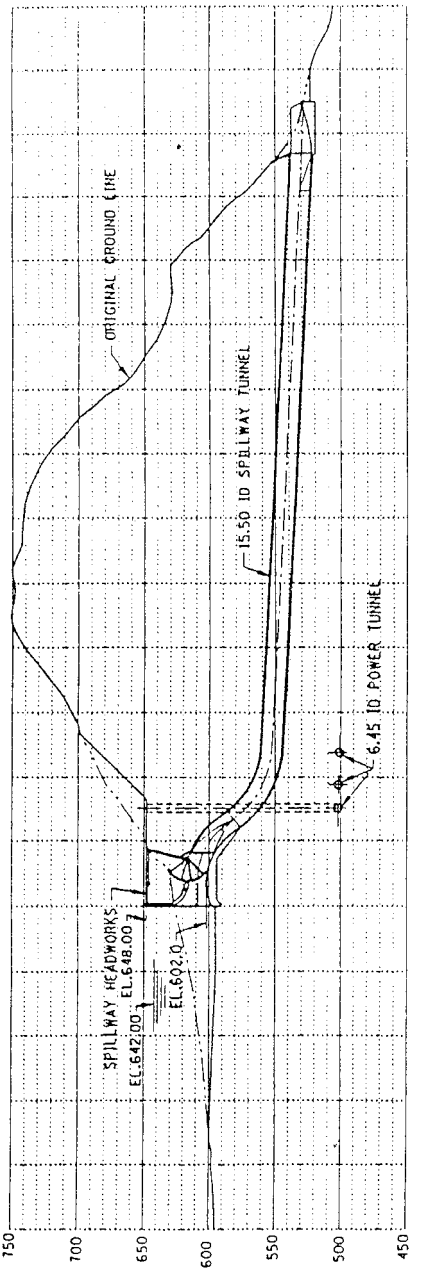

FIGURE 17.28 Typical arrangement of a tunnel spillway. (Harza Engineering Co., 1996).

water and head losses up to and including the vertical bend, and uniform flow at a depth of 75 percent with long-term tunnel roughness (assume Manning's $n = 0.016$) in the flat-tunnel section downstream.

If the head is sufficient to produce a velocity of 25 to 30 m/s at the end of the vertical curve, an aeration ramp must be provided upstream of the curve. The location and geometry of the aeration ramp generally are determined by a physical model because of the circular shape of the tunnel.

17.9.3 Flat-Tunnel Section

The *flat-tunnel section* is generally situated as low as possible to minimize the tunnels size while maintaining the downstream end above the tailwater. If the downstream end is fixed—say, 3 meters above maximum tailwater—then the tunnel's size and slope are proportioned to produce a depth and velocity at the vertical bend that is consistent with headwater and energy losses in the entrance structure and the inclined shaft. In some cases, the length of the tunnel may be such that the downstream tunnel extends directly head and to the entrance structure without an inclined tunnel section. In such a case, the aeration ramp would be placed in the down stream tunnel if the velocity reaches approximately 25 to 30 m/s.

It is most convenient for hydraulics and construction if the tunnel section has a square bottom, which provides more flow area and simplifies the design of the aeration ramp. It also eliminates the transition from the downstream tunnel to the flip-bucket.

17.9.4 Flip-Bucket

The energy dissipator for a tunnel spillway will almost always be a *flip-bucket* because it is generally the most economical solution. Any transition from the tunnel to the flip-bucket must be gradual. The simplest flip-bucket is the straight cylindrical type that has the same width as does the tunnel. However, if the impact of the jet with the tailrace is not acceptable, a special bucket may be required. Such a bucket might turn or spread the flow, to limit or localize the plunge-pool scour. A special bucket generally requires a physical model. Because the tunnel spillway, as a general rule, will have special features, a physical model is usually recommended.

17.10 SPILLWAY CHUTE

17.10 .1 Smooth Chute

The *spillway chute* connects the crest structure with an energy dissipator. In plan, it may be straight or curved, have a uniform width, or be tapered. The most common design is a straight chute with a gradual taper. More complex designs require physical model tests. In section, it can have a uniform slope or have more than one slope connected by vertical curves. The most common chute profile is a flat upper chute and a steep lower chute connected by a vertical curve. Chute friction losses are generally calculated assuming that the minimum Manning's $n = 0.010$ (for energy dissipator design) and that the maximum Manning's $n = 0.016$ (for wall heights)

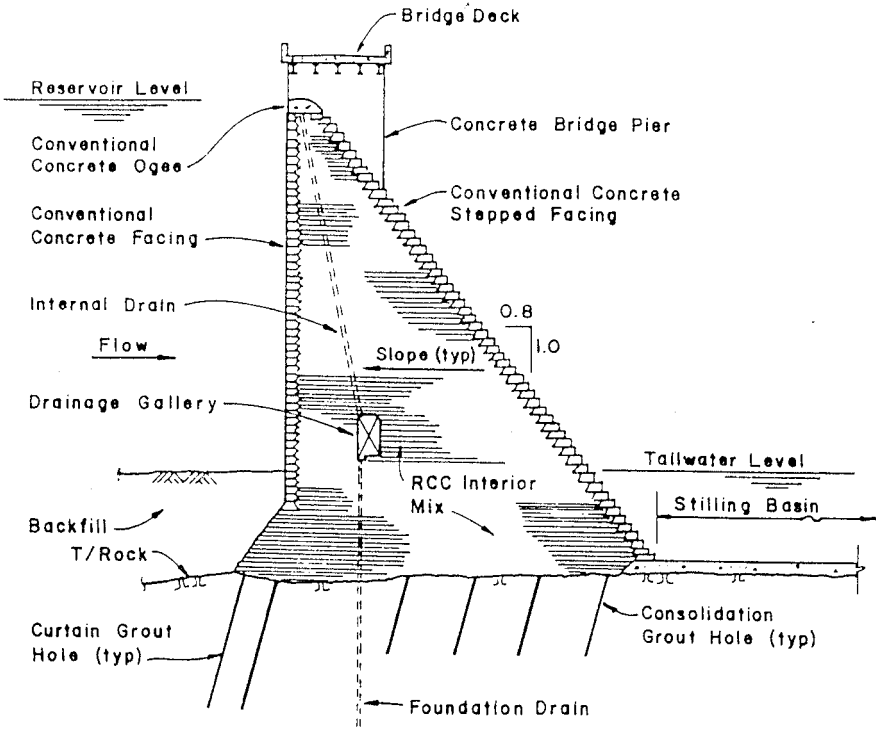

FIGURE 17.29 Typical RCC spillway section with stepped chute. (Zipparro and Hansen, 1993)

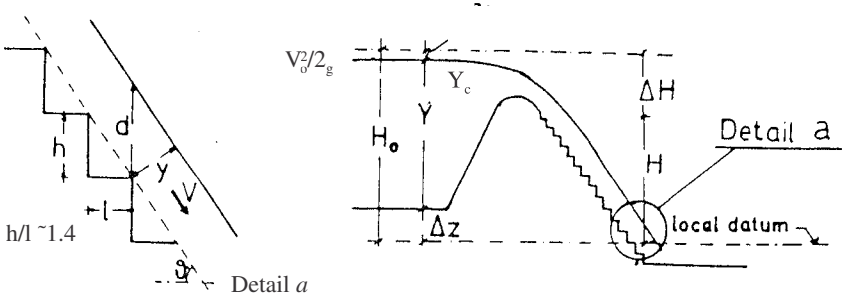

FIGURE 17.30 Notation sketches of a stepped chute: (Christodoulou, 1993)

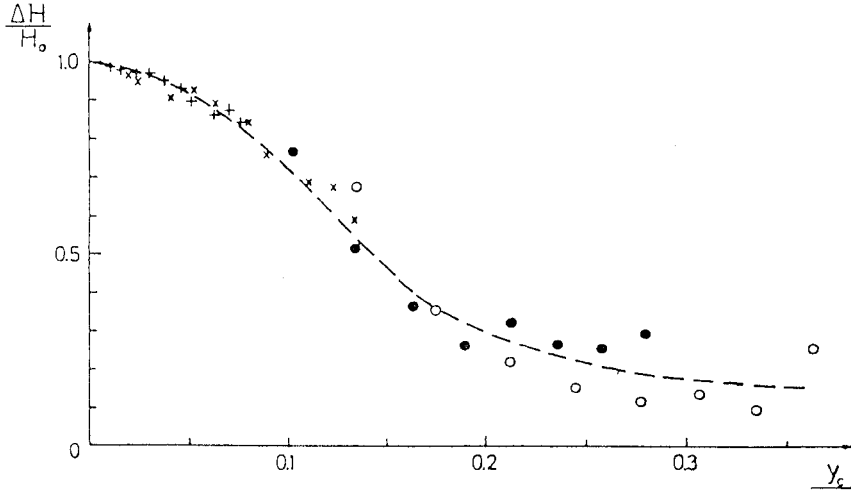

Figure 17.31 Relationship between head loss and critical depth for a stepped-chute spillway. (Christodoulou, 1993)

Side-wall freeboard can be taken as 20% of the calculated depth for a straight chute and 30% of calculated depth for a gradually tapered chute (3° maximum, each wall). For curved chutes, model studies are required. When chutes are gated, without interior divide walls, models are required to check ride-up of the flow on walls from nonuniform gate operations. Interior divide walls are sometimes used to separate normal-release bays from flood-release bays. The divide walls are normally sized for some part-gate condition to limit their height and cost.

17.10.2 Stepped Chutes

With the introduction of roller-compacted concrete dams, it has become convenient to leave steps on the downstream face of the spillway sec. (RCC) of a gravity dam. The steps not only save money on the chute but also dissipate energy that would remain to be dissipated by the stilling basin at the base of the dam (Zipparro and Hasen, 1993). Fig. 17.29 is a typical spillway section in a roller-compacted concrete dam. The design procedure for hydraulic design of the spillway is as follows:

1. Set the ungated crest length so that the maximum crest head is no more than 10 ft. (3 m).
2. Shape the ogee in accordance with Step 9. in Sec. 17.2.
3. Set the step height so that the ratio of critical depth at the crest over the step height is $y_c/h < 4$ (Fig. 17.30).
4. Determine the head loss from headwater to stilling basin level based on Figs. 17.30 and 17.31.(N = number of steps).
5. Size the stilling basin in accordance with Chap. 18.

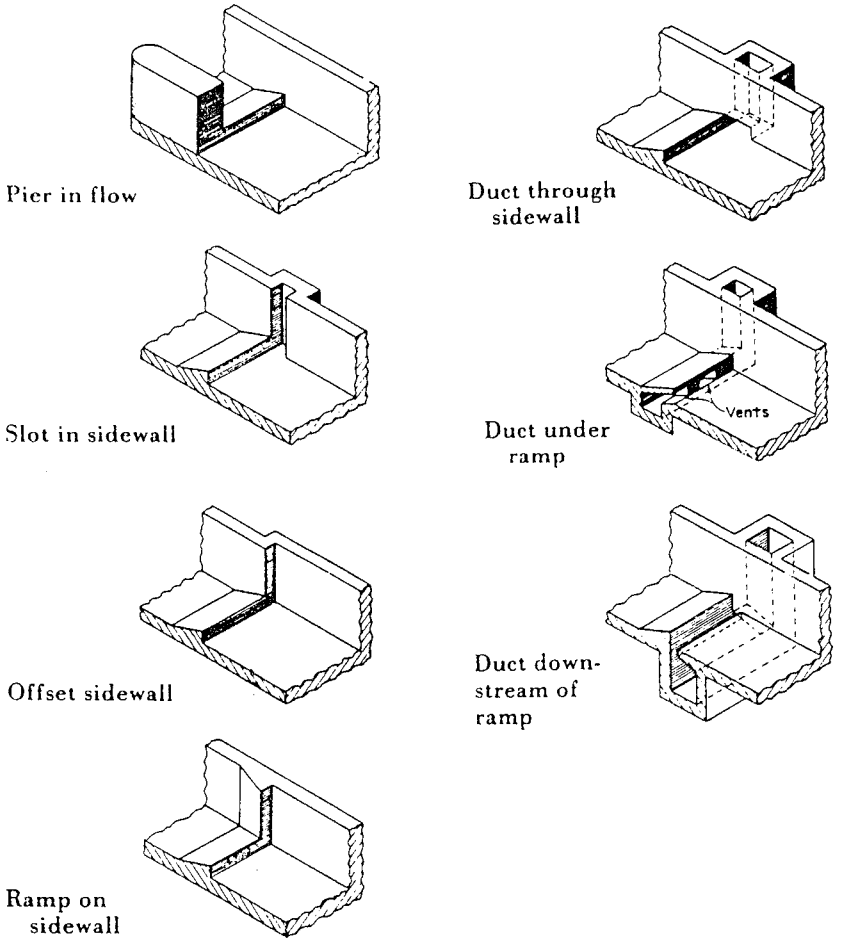

Figure 17.32 Aeration ramps and air supply systems. (Falvey, 1990).

17.11 SPILLWAY AERATION RAMPS

In recent years, aeration has become the standard for cavitation protection for spillways (as well as for outlet works and other release facilities) for structures with a height greater than 50 m (Falvey, 1990; ICOLD, 1992; USACE, 1995; Zipparo and Hasen, 1993). Aeration ramps of various types have been used on spillway chutes (Fig. 17.32) as well as on tunnel spillways (Fig. 17.33). Air is supplied to the ramps in various ways (Fig. 17.32).

The aeration ramp requirement is generally determined on the basis of an assessment of the cavitation potential along the entire length of the spillway. The cavitation potential can be expressed in terms of the cavitation number (or cavitation index) σ as

$$\sigma = \frac{p_o - p_v}{\rho_w \frac{V_o^2}{2g}} \tag{17.12}$$

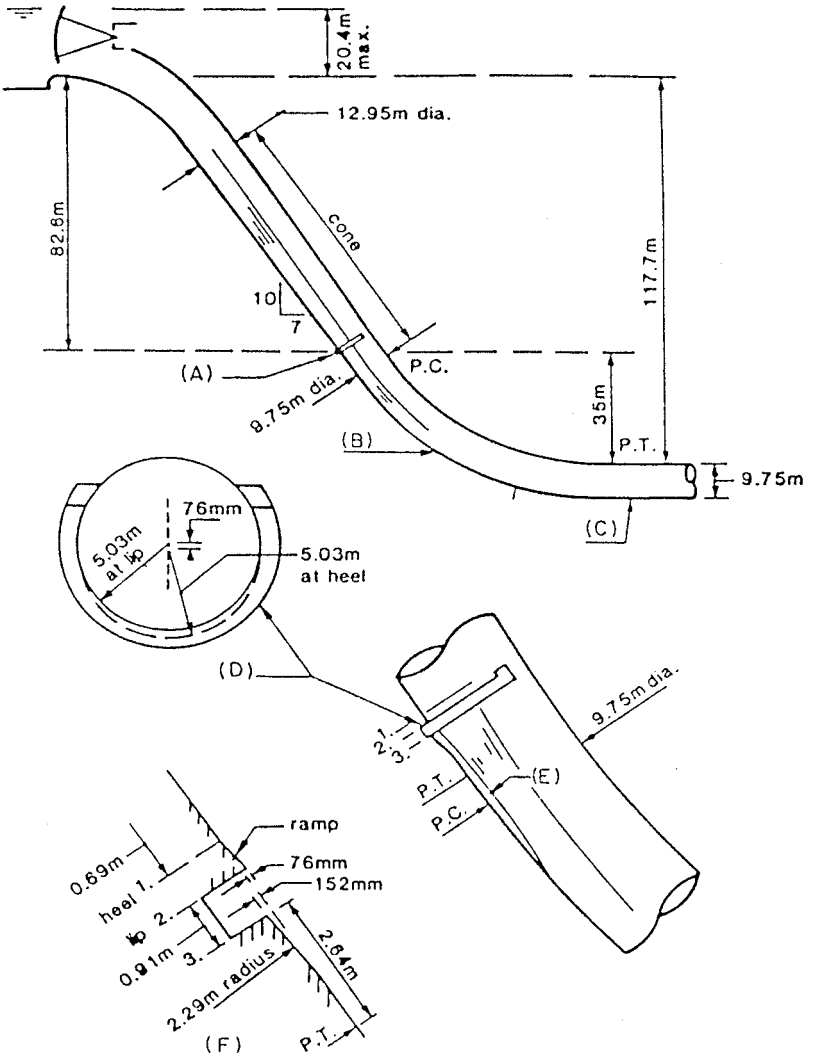

(A) Air trough.

(B) Area of minor damage.

(C) Area of major damage.

(D) Horse-shoe trough.

(E) Air cavity.

(F) Detail of air trough along axis of invert.

Figure 17.33 Aeration ramp and slot of the Yellowtail Dam tunnel spillway. (ICOLD, 1992)

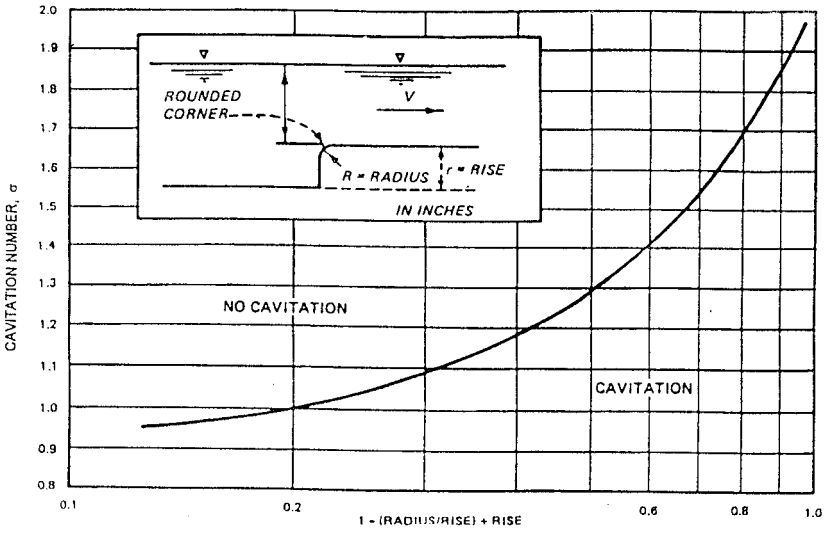

C

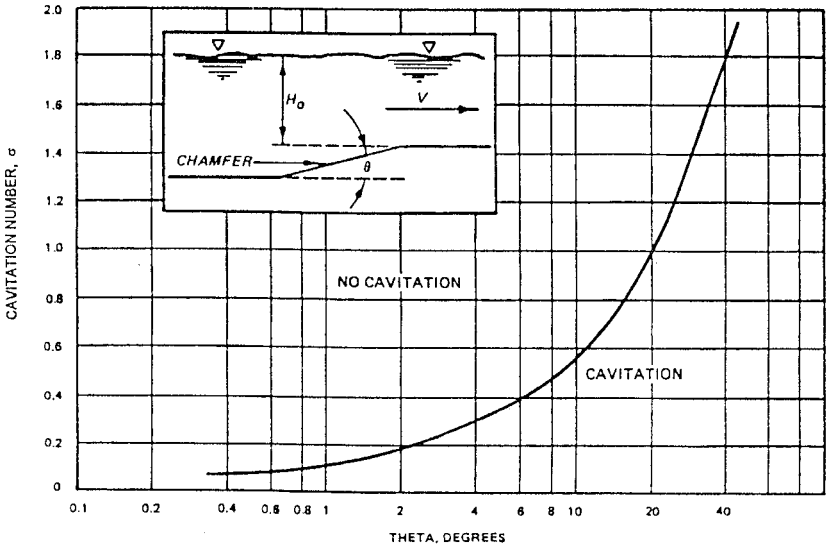

D

FIGURE 17.34 Cavitation Characteristics of Local Irregularities. (continued).

where $p_o = p_a + p_g$ = reference pressure, p_a = atmospheric pressure, p_g = gauge pressure, p_v = vapor pressure of water, ρ_w = density of water, and V_o = reference velocity.

In general, cavitation damage is expected, at locations where the value of the cavitation number is less than 0.2. In addition to the flow velocity and depth, the occurrence of cavitation damage also depends on the expected or existing local irregularities in the spillway's surface, the strength of the surface material, the elevation of the structure, and the length of operation. For a specific surface irregularity, the critical cavitation number can be determined from Fig. 17.34. An aeration ramp separates the flow from the boundary and forms a cavity so that air can be entrained underneath the surface of the free jet to provide protection against cavitation damage. Since the cavitation number depends on the local velocity and pressure, the maximum discharge is not necessarily the flow rate that produces the highest cavitation potential or the lowest value of the cavitation number of the flow.

Aeration ramps for tunnels must be verified by a physical model unless an extremely close approximation can be made to an existing design that has been model tested. However, aeration ramps for chute spillways can largely be designed using computer models because the flow is primarily two-dimensional (Brater et al., 1996; DeFazio and Wei, 1983; Falvey, 1990; ICOLD, 1992; Wei and DeFazio, 1982; Zipparo and Hasen, 1993). Brief descriptions of several computer models for analysis of spillway aeration ramps can be found in Brater et al. (1996). However, if significant three-dimensional effects are produced by a flat chute slope or tapered side walls, where return flow or accumulation of flow in the cavity beneath the jet might reduce the effective jet trajectory, the design should be confirmed by physical model tests.

The recommended procedure for the design of ramp and air vent on a simple chute is as follows:

1. Perform an analysis of the spillway's water surface profile for flows up to the maximum discharge in approximately 20-percent increments.
2. For the preliminary assessment, find the upstream-most site where the mean velocity is approximately 30 m/s for maximum discharge and where protection by aeration is likely to be needed. Experience has shown that significant cavitation damage usually will not occur upstream of this point.
3. Determine the cavitation numbers for the entire length of the spillway for each flow rate based on the flow velocities and depths obtained in Step 1. The computer program provided in Falvey (1990) can be used.
4. Determine the upstream-most site where the computed value of the cavitation number is less than 0.20, or the critical cavitation number for the expected local irregularities, and find an appropriate site for the first ramp so that the impact point of the jet is at the desired location.
5. Based on a consideration of the frequency and discharges of the spillway operation, each ramp should be sized to draw quantity of air equal to approximately 10% of the maximum water flow.
6. The required cavity length L for maximum flow can then be determined using the following equation (see also Fig. 17.35):

$$q_a = 0.022\ VL \tag{17.13}$$

where q_a = air discharge per unit width, V = mean water velocity approaching the ramp, and L = cavity length.

7. Use a computer model to determine a suitable ramp geometry to provide the required cavity length L, assuming a free-jet underpressure of –1.0 m (water). The computer models described in Falvey (1990), Harza Engineering Co. (1996), and Wei and DeFazio (1982) can be used.
8. Size the air vent to provide the air flow from Step 6, with no more than –1.0 m under-pressure and an air vent velocity that does not exceed 80 m/s to avoid excessive noise and choking of the air flow.
9. Use the computer model to analyze the performance of the ramp/air vent for the full range of flow. If the resulting air vent velocity or underpressure exceeds the allowable 80 m/s or –1.0 m, respectively, resize the ramp to provide acceptable conditions over the full range of flows.
10. Place the succeeding ramps no more than 50 m apart. The last ramp should be no closer than approximately 20 m to the entrance to the energy dissipator (stilling basin or flip-bucket). Check the concentration of air downstream of the aeration ramp in accordance with the following equation (Falvey, 1990):

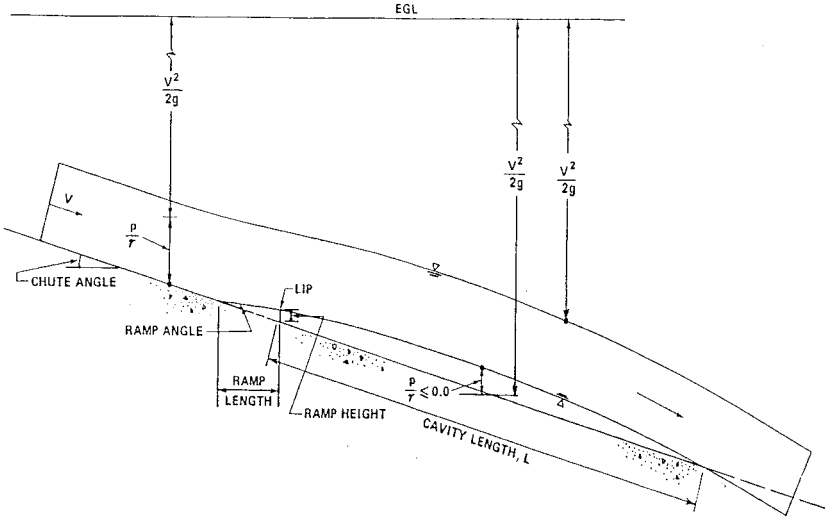

Figure 17.35 Definition sketch of a free-jet from an aeration ramp. (Wei and DeFazio, 1982)

(a)

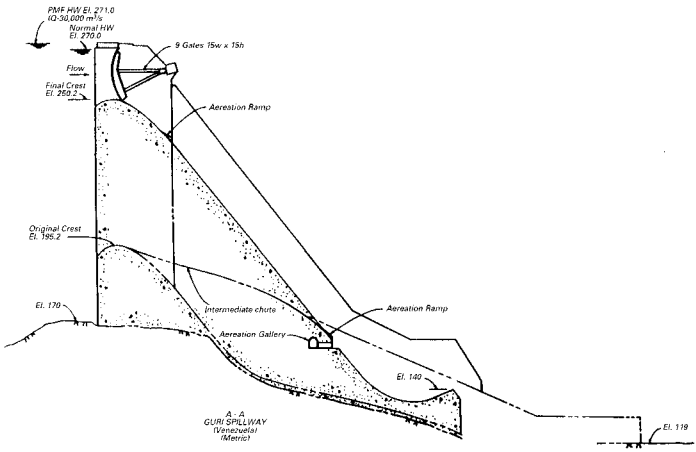

(b)

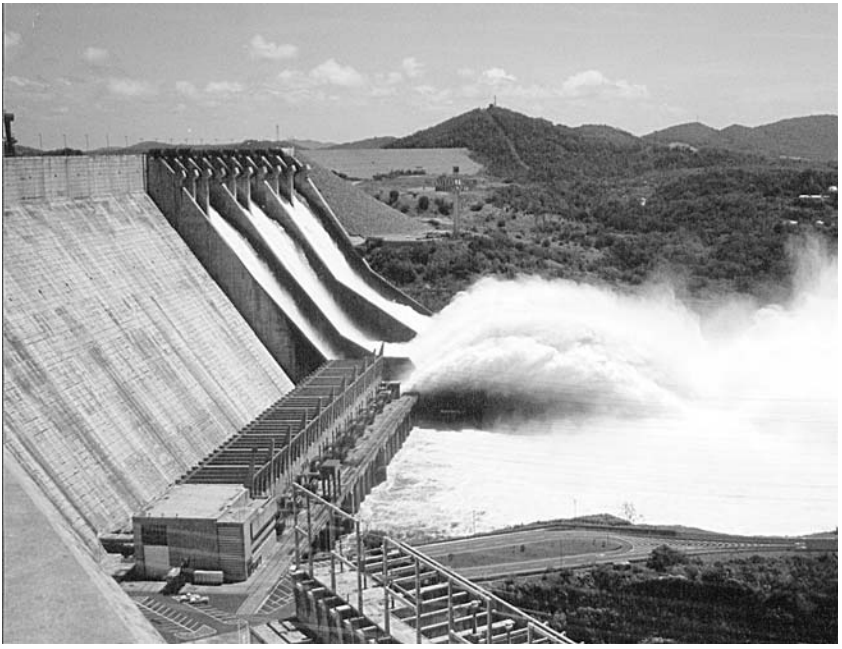

(c)

(d)

(e)

(f)

Exhibit 17.7 Guri hydroelectric project, Venezuela (Courtesy CVG–EDELCA, Caracas).
(a) General view of the spillway showing aeration ramps and flip buckets.
(b) Layout of the right spillway chute showing aerators and flip bucket.
(c) General view of the spillway in operation.
(d) Close–up view of the spillway in operation.
(e) Close–up view of the flow condition at an intermediate aeration ramp.
(f) Close–up view of flow separation at the end of a trestle pier for aeration.

$$C_x = C_o e^{-K(L_x - L_i)} \tag{17.14}$$

where C_X = mean air concentration at distance X, C_o = mean air concentration at beginning of aeration, L_X = slope distance downstream from aerator, L_i = slope distance downstream from aerator to beginning of aeration, and $K = 0.017$ = dimensional constant per meter (i.e., 0.017 m^{-1}). On a straight section, the concentration of air decreases approximately 0.15 to 0.20% per meter (Falvey, 1990).

11. Install the ramp design from Step 7, in a physical model, if necessary. The model should be 1:20 or larger and should include all geometric details that could reduce the effective jet trajectory. The ramp design might need adjustment as a result of the model studies. In the model, air flow will be reduced because of scale effects. Therefore, use the ramp underpressure as input in the computer model to confirm the jet trajectory.

Note that the above procedure is a rule-of-thumb approach based on experience over the past 30 years or so. Design of ramps over this period has varied significantly within the United States and around the world. Although considerable model information is available, prototype data are limited. The most critical piece of data relates air concentration at the chute's surface to distance downstream of the ramp. This determines the required spacing of ramps.

The other important criterion is how much air should be input at each ramp. Current thinking is that the concentration of air just downstream of the ramp should not exceed approximately 50% in the bottom flow layer. The guidelines above assume that the bottom 10% of depth should be equal parts of air and water.

Exhibit 17.7 illustrates a spillway aeration ramp.

17.12 SAMPLE DESIGN

Determine the geometry of the spillway crest and the discharge rating curve for an ungated overflow spillway. A bridge over the spillway will be supported on piers 1.8 m thick, with a maximum span width of 12 m between the centerline of piers. The reservoir and flood data are as follows:

Maximum flood discharge	=	2800 m^3/sec
Maximum flood pool elevation	=	110 m
Maximum normal pool elevation	=	100 m
Approach channel invert elevation	=	80 m
Downstream channel elevation	=	20 m
Maximum flood tailwater elevation	=	40 m

Assume that the overflow crest becomes tangent to a spillway chute that is slopes at 1*h*:1*v*.

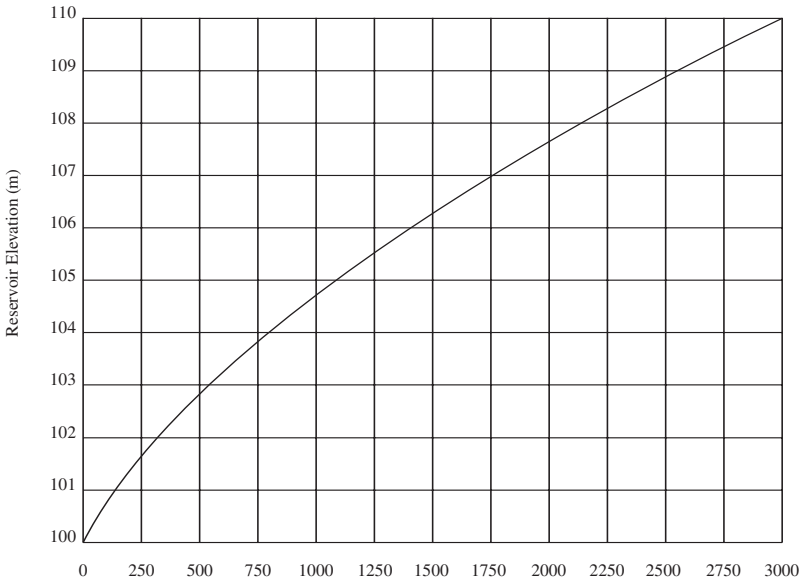

FIGURE 17.36 Spillway discharge rating curve.

17.12.1 Design Head

In this example, the spillway crest elevation is the same as the normal maximum pool elevation, and the maximum head available to pass the maximum flood discharge is $H_{MAX} = 110 - 100 = 10$ m. The design head H_0 will be selected as $H_0 = 0.8H_{MAX} = 8$ m. By selecting a design head that is less than the maximum head, there will be a region of negative pressure on the spillway crest during the maximum discharge, which results in an increased discharge coefficient. Negative pressure is acceptable during maximum discharge provided that it does not exceed one-half atmosphere.

17.12.2 Discharge Coefficient

The basic discharge coefficient C_0 is determined using Fig. 17.1.

$P = 100 - 80 = 20$ m

$P/H_0 = 20/8 = 2.5$

$C_0 = (0.552)(3.945) = 2.178$

Figure 17.2 is used to determine discharge coefficients for a range of heads to complete the discharge rating curve (Fig. 17.36).

This spillway will have a vertical upstream face. Since the maximum tailwater elevation is well below the spillway crest, there will be no tailwater effect and no apron effect.

No further corrections to the discharge coefficient will be required.

17.12.3 Crest Length

Pier nose shape Type 3A from Fig. 17.6 is selected for the bridge piers. The pier contraction coefficient K_p can be assumed to be 0.0. The headwall will be 90° to the direction of flow with rounded abutments. $K_a = 0.1$

$H_{MAX}/H_0 = 1.25$

$C_{MAX}/C_0 = 1.03$ (Fig. 17.2)

$C_{MAX} = (1.03)(2.178) = 2.243$

$Q_{MAX} = C_{MAX}LH_{MAX}^{3/2} = (2.243)L(10)^{3/2} = 2800$ m³/s

$L = 39.48$ m

Three piers will be required to support the bridge. The net length of the crest L' is determined from L = L' – 2(0.1)(10) = 39.48 m L' = 41.48 m (use four bays at 10.5 m each). The total spillway crest length, including three piers at 1.8 m thickness, is 47.4 m.

17.12.4 Checking Minimum Pressure on the Crest

From Figs. 17.7 and 17.8 the minimum pressure at maximum discharge (H/Hd = 1.25) occurs along the pier and is about –2.8 m, which is less than one-half atmosphere or 5 m head. This is acceptable.

17.12.5 Discharge Rating Curve

The discharge rating curve is developed in the following table:

Elevation	H_e	H_e/H_0	C/C_0	C	L	Q
100.0	0.0	0.0	0.78	1.70	42.0	0
101.0	1.0	0.125	0.83	1.81	41.8	76
102.0	2.0	0.250	0.87	1.89	41.6	223
103.0	3.0	0.375	0.89	1.94	41.4	417
104.0	4.0	0.5	0.92	2.00	41.2	660
105.0	5.0	0.625	0.95	2.07	41.0	948
106.0	6.0	0.25	0.97	2.11	40.8	1267
107.0	7.0	0.825	0.99	2.16	40.6	1621
108.0	8.0	1.0	1.00	2.18	40.4	1991
109.0	9.0	1.125	1.02	2.22	40.2	2411
110.0	10.0	1.25	1.03	2.24	40.0	2838

Source:Plot of Discharge Rating Curve

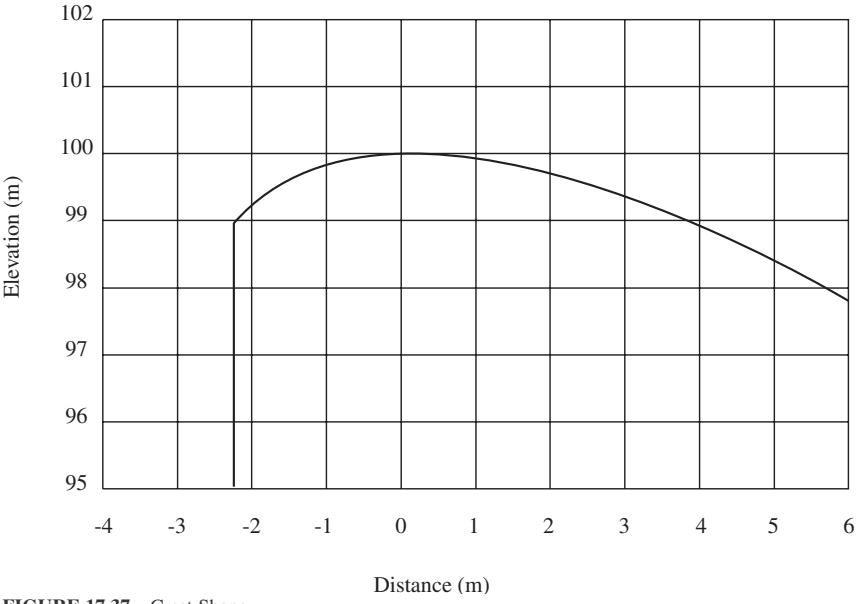

FIGURE 17.37 Crest Shape

17.12.6 Crest Geometry

Unit discharge approaching crest at design head H_0 = 8m:
q = 1991/47.4 = 42 m³/s/m.
Approach velocity:
$V_a = q/(P + H_0)$ = 42/28 = 1.5 m/s.
Approach velocity head:
h_a = 0.115 m
and h_a/H_0 = 0.014.

Parameters for the crest geometry are determined from Fig. 17.9.

K = 0.503
N = 1.865
X_c/H_0 = 0.277
Y_c/H_0 = 0.12
R_1/H_0 = 0.525
R_2/H_0 = 0.225

The origin of the X-Y axis is at the crest of the spillway, and X_c is the distance from the upstream face to the crest.
Upstream of the origin:

$X_c = 2.216$ m,

$Y_c = 0.960$ m,

$R_1 = 4.200$ m, and

$R_2 = 1.800$ m.

Downstream of the origin:

$Y = -0.08325\ X^{.865}$

Location of the tangent point is determined by

$Y' = -0.08325(1.865)X^{0.865} = -1.0$

$X_t = 8.614$

$Y_t = 4.619$

The crest geometry is plotted on Fig. 17.37.

Plot of crest geometry.

REFERENCES

Ackers, P., and A. R. Thomas, "Design and Operation of Air-Regulated Siphons for Reservoir and Head-Water Control," *Proceedings of the Symposium on Design and Operation of Siphons and Siphon Spillways*, London, UK, May 1975.

Brater, E. F., H. W., King, J. E. Lindell, and C. Y. Wei, *Handbook of Hydraulics*, 7th ed., McGraw-Hill, New York, 1996.

Chow, V. T., *Open-Channel Hydraulics*, McGraw-Hill, New York, 1966.

Christodoulou, G. C., "Energy Dissipation on Stepped Spillways," *Journal of Hydraulic Engineering*, *ASCE,* 119, (5): May 1993.

Coleman, H. W., "Prediction of Scour Depth from Free Falling Jets," *Proceedings, of the ASCE Hydraulics Division Conference on Applying Research to Hydraulic Practice*, Jackson, Ms, 1982,

DeFazio F. G., and C. Y. Wei, "Design of Aeration Devices on Hydraulic Structures," Frontiers in Hydraulic Engineering, American Society of Civil Engineers, New York, 1983.

Falvey, H. T., *Cavitation in Chutes and Spillways*, USBR Engineering Monograph No. 42, USBR, 1990.

Harza Engineering Co., Internal Report, July 1996.

Hinchliff D. L., and K. L. Houston, *Hydraulic Design and Application of Labyrinth Spillways*, Research Engineering and Research Center, U.S. Bureau of Reclamation, 1984.

ICOLD, *Spillways, Shockwaves and Air Entrainment—Review and Recommendations*, Bulletin No. 81, ICOLD, Paris, 1992.

ICOLD, "Spillways for Dams," Bulletin No. 58, ICOLD, Paris, 1987.

Institute of Civil Engineers, "Mangla," *Proceedings of the Institute of Civil Engineers*, Binnie & Partners, Westminster, 1968.

Tacail, F. G., B. Evans, and A. Babb, "Case Study of a Labyrinth Weir Spillway," *Canadian Journal of Civil Engineering*, 17, 1990.

Tullis, J. P., N. Amanian, and D. Waldron, "Design of Labyrinth Spillways," *Journal of Hydraulic Engineering*, *ASCE* 121 (3): March 1995.

USACE, *Hydraulic Design of Spillways*, U.S. Army Corps of Engineers, No. EM 1110-2-1603, American Society of Civil Engineers, New York, 1995.

USACE, *Hydraulic Design Criteria*, U.S. Army Corps of Engineers Waterways Experiment Station, Vicksburg, Ms, 1988.

USBR, *Design of Small Dams*, U. S. Bureau of Reclamation, Denver, CO, 1987.

Vischer, D. L., and W. H. Hager, Energy Dissipators—Hydraulic Design Considerations, IAHR Hydraulic Structures Design Mannual No. 9, A. A. Balkema, Rotterdam, Netherlands, 1995.

Wei, C. Y., and F. G. DeFazio, "Simulation of Free Jet Trajectories for the Design of Aeration Devices on Hydraulic Structures," *Proceedings of the 4th International Conference on Finite Elements in Water Resources*, Hannover, Germany, June 1982.

Whittaker, J. G., and A. Schleiss, "Scour Related to Energy Dissipators for High Head Structures," Nr. 73, Mitteilungen der Versuchsanstalt fur Wasserbau, Hydrologie und Glazioloie, Zurich, 1984

Zipparro, V. J., and H. Hasen, *Davis' Handbook of Applied Hydraulics*, 4th ed., McGraw-Hill, New York, 1993.